

Author	Degree	Prof.
	Given Name	Vladimir
	Particle	
	Family Name	Dobrokhodov
	Suffix	
	Phone	001 831-656-7714
	Fax	
	Email	vldobr@nps.edu, vldobr@gmail.com
Affiliation	Division	Mechanical and Aerospace Engineering Department
	Organization	Naval Postgraduate School
	Street	699 Dyer, Halligan Hall, Bldg 234
	Postcode	93943
	City	Monterey
	State	CA
	Country	USA

## Abstract

This chapter provides a review of basic knowledge required for accurate mathematical modeling of flight of a fixed-wing UAV. These include the kinematics and dynamics of motion and the transformation of forces and moments acting on the airplane. The detailed discussion of the “kinematics–dynamics–actions” triad in application to a generic fixed-wing UAV is the main objective of this chapter. Therefore, the presentation starts with an introduction to the coordinate frames, their transformations, and differential rotations. Kinematics of the coordinate frames is what connects states of a fixed-wing UAV and transforms forces and moments acting in different coordinate frames. Understanding of reference frames and their dynamics is essential for the guidance, navigation, and control systems design. Next, the chapter provides a detailed derivation of the equations of motion using the Newtonian approach. Assuming that a fixed-wing UAV can be represented as a rigid body moving in an inertial space allows for the derivation of the linear and angular momentum equations. Starting in an inertial frame, it is shown how the final form of translational and rotational equations of motion becomes written in a body-fixed coordinate frame. The development of both the kinematic and dynamic equations is carried out first in a general vector form; then, using simplifying assumptions applicable to a generic fixed-wing symmetric UAV, the vector equations are expanded into a scalar form to better represent the physical meaning of their components. Finally, the chapter presents the principles of defining the external forces and moments acting on a generic fixed-wing airplane. Since the forces and moments found on an airplane act in a number of coordinate frames including inertial, body-fixed, and wind frames, the chapter utilizes the concepts and tools built in the kinematics section to transform the forces and moments into the body-fixed frame. Such transformations complete the presentation of the “kinematics–dynamics–actions” triad.

---

# Kinematics and Dynamics of Fixed-Wing UAVs

53

Vladimir Dobrokhodov

## Contents

53.1	Introduction .....	2
53.2	Reference Frames and Coordinate Transformations .....	3
53.2.1	Kinematics of Moving Frames .....	4
53.2.2	Generalized Motion .....	9
53.2.3	Coordinate Frames .....	11
53.3	Rigid Body Dynamics .....	19
53.3.1	Conservation of Linear Momentum .....	19
53.3.2	Conservation of Angular Momentum .....	22
53.3.3	Complete Set of 6DoF Equations of Motion .....	25
53.4	Forces and Moments Acting on the Airplane .....	26
53.4.1	Gravitation .....	26
53.4.2	Propulsion .....	27
53.4.3	Unsteady Atmosphere .....	28
53.4.4	Aerodynamics .....	28
53.5	Accounting for the Earth Rotation Rate .....	32
53.6	Conclusion .....	35
	References .....	35

## Abstract

This chapter provides a review of basic knowledge required for accurate mathematical modeling of flight of a fixed-wing UAV. These include the kinematics and dynamics of motion and the transformation of forces and moments acting on the airplane. The detailed discussion of the “kinematics–dynamics–actions” triad in application to a generic fixed-wing UAV is the main objective of this chapter. Therefore, the presentation starts with an introduction to the coordinate frames, their transformations, and differential rotations. Kinematics of the coordinate

V. Dobrokhodov  
Mechanical and Aerospace Engineering Department, Naval Postgraduate School, 699 Dyer,  
Halligan Hall, Bldg 234, 93943, Monterey, CA, USA  
e-mail: [vldobr@nps.edu](mailto:vldobr@nps.edu), [vldobr@gmail.com](mailto:vldobr@gmail.com)

AU1

K.P. Valavanis, G.J. Vachtsevanos (eds.), *Handbook of Unmanned Aerial Vehicles*,  
DOI 10.1007/978-90-481-9707-1\_53, © Springer Science+Business Media Dordrecht 2013

1

frames is what connects states of a fixed-wing UAV and transforms forces and moments acting in different coordinate frames. Understanding of reference frames and their dynamics is essential for the guidance, navigation, and control systems design. Next, the chapter provides a detailed derivation of the equations of motion using the Newtonian approach. Assuming that a fixed-wing UAV can be represented as a rigid body moving in an inertial space allows for the derivation of the linear and angular momentum equations. Starting in an inertial frame, it is shown how the final form of translational and rotational equations of motion becomes written in a body-fixed coordinate frame. The development of both the kinematic and dynamic equations is carried out first in a general vector form; then, using simplifying assumptions applicable to a generic fixed-wing symmetric UAV, the vector equations are expanded into a scalar form to better represent the physical meaning of their components. Finally, the chapter presents the principles of defining the external forces and moments acting on a generic fixed-wing airplane. Since the forces and moments found on an airplane act in a number of coordinate frames including inertial, body-fixed, and wind frames, the chapter utilizes the concepts and tools built in the kinematics section to transform the forces and moments into the body-fixed frame. Such transformations complete the presentation of the “kinematics–dynamics–actions” triad.

### 53.1 Introduction

The chapter objective is to provide an overview of the necessary theoretical material to enable a reliable mathematical modeling of the free and controlled motion of a generic fixed-wing UAV. Although the subject is not new and is well presented in existing literature, the rapid advancements of the last decade in research and development of fixed-wing UAV technologies open new applications that require understanding and a careful application of the existing assumptions. New materials, novel structural designs, new aerodynamic configurations, and advanced onboard instrumentation including miniature sensors, actuators, and tremendous onboard processing power enable much wider operational envelop of fixed-wing UAVs and significantly higher utility of their payloads. Depending on the UAV configuration and its intended operational use, the standard 12 equations of motion might not suffice for the task at hand and require deeper consideration of the UAV components interaction.

This chapter starts with some preliminaries required to describe kinematics of a rigid body motion in three-dimensional (3D) space. Thus, the kinematics of 3D rotation is introduced first. The most commonly used coordinate frames that are utilized in the description of UAV states are presented next. Applying the kinematics of rotating frames to a set of specific coordinate frames builds the basis for a convenient description of the external forces and moments acting on a fixed-wing airplane. Understanding of reference frames and their rotations is essential for the eventual development of the guidance, navigation, and control systems architecture.

73 Next, the chapter provides a detailed derivation of the equations of motion using the  
 74 classical Newtonian approach. Assuming that a fixed-wing UAV can be represented  
 75 as a rigid body moving in an inertial space allows for the derivation of the linear  
 76 and angular momentum equations. Starting in an inertial frame, it is shown how  
 77 the final form of translational and rotational equations of motion can be written  
 78 in a body-fixed coordinate frame. The development of both the kinematic and  
 79 dynamic equations is carried out first in a general vector form, and then, using  
 80 simplifying assumptions applicable to a generic fixed-wing symmetric UAV, the  
 81 vector equations are expanded into a scalar form to better highlight the physical  
 82 meaning of their components. Since the external forces and moments found on an  
 83 airplane act in a number of coordinate frames including inertial, body-fixed, and  
 84 wind frames, the chapter utilizes the concepts and tools built in the kinematics  
 85 description to transform the forces and moments into the body-fixed frame. Thus,  
 86 the complete derivation of linear and angular momentum equations, along with the  
 87 forces and moments acting on a rigid body, results in the generalized set of 6 degrees  
 88 of freedom (6DoF) equations of motion.

AU2

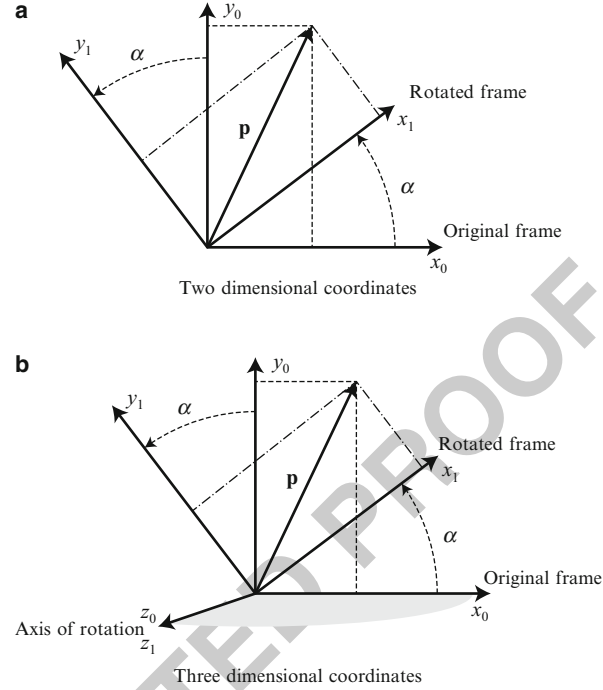
## 89 53.2 Reference Frames and Coordinate Transformations

90 In order to accurately describe a body motion, it is required to define (i) the forces  
 91 and moments acting on the body and thus resulting in the body motion and (ii) the  
 92 coordinate system that can be used as a reference for the motion states definition. It  
 93 is important to note that there are two types of forces acting on a body in free motion:  
 94 first, the inertial forces and moments that depend on the velocities and accelerations  
 95 relative to an inertial reference frame; the classical Newtonian dynamics equations  
 96 hold only in the inertial frame. The second group consists of the aerodynamic  
 97 forces and moments resulting from interaction of the body with the surrounding  
 98 airflow and therefore relative to the air. Since the airflow might not be stationary,  
 99 it is therefore convenient to describe the resulting aerodynamics in the coordinate  
 100 frames connected to the body and to the surrounding air. The resulting motion can be  
 101 conveniently described in terms of the position, velocity, acceleration, and attitude  
 102 coordinates which comprise the states of the moving body. Some of these states, in  
 103 turn, need to be defined with respect to a reference frame which choice is defined  
 104 by the specifics of the UAV application. Thus, the information carried by various  
 105 reference frames is what facilitates the complete and convenient definition of the  
 106 free body motion.

AU3

107 Therefore, this section starts with a definition of a coordinate frame and the  
 108 description of the coordinate frame rotation. The reference frames required to  
 109 represent the aerodynamic forces and moments and facilitating the solution of the  
 110 navigation states are introduced next. Communication of the states information  
 111 occurring during the coordinate frame transformation is presented for the major  
 112 coordinate frames typical for UAV applications. The section ends with a set of  
 113 kinematic equations required to represent the transition of linear and angular  
 114 accelerations.

**Fig. 53.1** The same plane rotation considered with respect to two and three axes.  
(a) Two-dimensional coordinates. (b) Three-dimensional coordinates



### 53.2.1 Kinematics of Moving Frames

The objective of this subsection is to define a coordinate frame transformation and the associated mathematical formalism. Namely, the direct cosine matrix (DCM) is introduced, and its key properties are presented. The DCM matrix formalism is then followed by a differential rotation that defines the rate of change of the DCM matrix. A fundamental property of the simple summation of angular rates is introduced next. The section ends with a detailed presentation of the coordinate frames used to describe the 6DoF motion of a rigid body. The results of this development are heavily utilized throughout the entire chapter.

An arbitrary motion of a rigid body can be described by a transformation that consists of (Goldstein 1980) translational and rotational components. First, a pure rotation of a rigid body is addressed. Consider a vector  $\mathbf{p}$  defined in two orthogonal coordinate frames rotated with respect to their mutual origin by angle  $\alpha$ , as shown in Fig. 53.1a.

From this geometrical setup, it can be demonstrated that vector  $\mathbf{p} = [x_0, y_0]$  can be uniquely defined in both frames as follows:

$$\begin{aligned} x_1 &= x_0 \cos \alpha + y_0 \sin \alpha \\ y_1 &= -x_0 \sin \alpha + y_0 \cos \alpha \end{aligned} \quad (53.1)$$

where 0 and 1 subscripts refer to the coordinates of  $\mathbf{p}$  in the original and rotated frames correspondingly.

Introducing the matrix notation for the linear transformation above results in a simple form that relates the vector  $\mathbf{p}$  components in  $(x_0, y_0)$  frame to the corresponding components in  $(x_1, y_1)$  frame:

$$\begin{bmatrix} x_1 \\ y_1 \end{bmatrix} = R_0^1 \begin{bmatrix} x_0 \\ y_0 \end{bmatrix}, \quad R_0^1 = \begin{bmatrix} \cos \alpha & \sin \alpha \\ -\sin \alpha & \cos \alpha \end{bmatrix}. \quad (53.2)$$

The resulting rotation matrix is called a DCM matrix. The DCM matrix  $R_0^1$  consists of the cosine and sine functions which are the direction cosines between the matching axes of the new and old coordinate systems denoted in the superscript and the subscript correspondingly. Following the same approach, it can be demonstrated that for the case of right-handed coordinate system represented by three orthogonal axes (see Fig. 53.1b), the same right-hand rotation results in transformation

$${}_z R_0^1 = \begin{bmatrix} \cos \alpha & \sin \alpha & 0 \\ -\sin \alpha & \cos \alpha & 0 \\ 0 & 0 & 1 \end{bmatrix}, \quad (53.3)$$

where for clarity, the subscript  $z$  denotes the axes of rotation. Proceeding similarly, right-handed rotations of the coordinate frame about the  $y_0$  and  $x_0$  axis give

$${}_y R_0^1 = \begin{bmatrix} \cos \alpha & 0 & -\sin \alpha \\ 0 & 1 & 0 \\ \sin \alpha & 0 & \cos \alpha \end{bmatrix}, \quad {}_x R_0^1 = \begin{bmatrix} 1 & 0 & 0 \\ 0 & \cos \alpha & \sin \alpha \\ 0 & -\sin \alpha & \cos \alpha \end{bmatrix}. \quad (53.4)$$

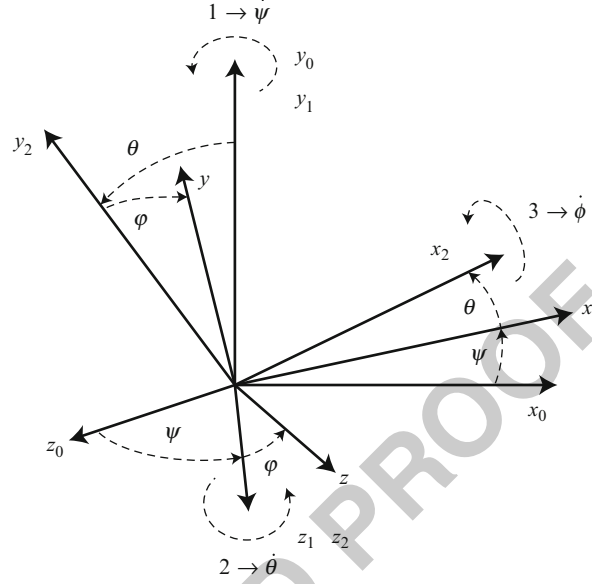
It is worth noting that the DCM transformation has the following easy-to-remember properties that simplify its application (see more details in Rogers 2003):

1. The transformed vector components along the axis of rotation remain unchanged with the rotation about that axis; elements of DCM are either 0 or 1.
2. The remaining elements of DCM are either sin or cos functions of the angle of rotation.
3. The cos elements are on the main diagonal with sin elements on off-diagonal.
4. The negative sin component corresponds to the component rotated “outside” of the quadrant formed by the original frames.
5. Columns (rows) of a DCM matrix form an orthonormal set.

It is straightforward to verify that a DCM matrix corresponding to the right-handed frames has the following properties:

$$\det(R) = 1; \quad R^T = R^{-1}; \quad R^T R = I; \quad R = [c_1, c_2, c_3] \Rightarrow c_i \cdot c_j = \begin{cases} 0, & i \neq j \\ 1, & i = j \end{cases} \quad (53.5)$$

**Fig. 53.2** Three consecutive rotations



162 and therefore it belongs to a general class of orthonormal transformation matrices.  
 163 For a sequence of rotations performed with respect to each orthogonal axis, the  
 164 resulting transformation can be obtained by a matrix composed of three sequential  
 165 rotations, called Euler angle rotations, starting from the original frame of reference;  
 166 see Fig. 53.2.

167 Formally, this transformation is accomplished by rotating through the ordered  
 168 sequence of Euler angles  $[\psi, \theta, \phi]$ , where the numerical indexes define the ordered  
 169 sequence of rotations and the corresponding axis of rotations:

$$170 \quad R_{x_0}^y = R_{x_2}^y R_{x_1}^{x_2} R_{x_0}^{x_1} \quad (53.6)$$

171 It is worth mentioning that the corresponding Euler angles are also widely used  
 172 to express elementary rotation matrices so that in (53.6), the following notation  
 173  $R_\phi = R_{x_2}^y, R_\theta = R_{x_1}^{x_2}, R_\psi = R_{x_0}^{x_1}$  is possible. As an example,  $R_\psi = R_{x_0}^{x_1}$  defines a  
 174 rotation of the axis  $x_0$  to  $x_1$  and  $z_0$  to  $z_1$  performed with respect to the axis  $y_0$  by the  
 175 angle  $\psi$ . From now, the same approach to denoting the rotations and vectors is used  
 176 throughout this chapter. In the case of rotations, the subscript refers to the original  
 177 frame while the superscript refers to the rotated frame; in the case of vectors denoted  
 178 in bold face, the subscript defines the frame where the vector is resolved and the  
 179 superscript refers to a specific meaning of the vector when necessary, and the frames  
 180 are indicated by the brace as in  $\{frame\}$ . Therefore, a vector  $\mathbf{p}_0 = [x_0, y_0, z_0]^T$   
 181 given in  $\{0\}$  coordinate frame can be resolved in another coordinate frame  $\{1\}$  of  
 182 arbitrary orientation with respect to the original frame by a transformation matrix  
 183  $R_0^1$  composed of three sequential rotations as follows:



$$\begin{bmatrix} x_1 \\ y_1 \\ z_1 \end{bmatrix} = \underbrace{\begin{bmatrix} 1 & 0 & 0 \\ 0 & \cos \phi & \sin \phi \\ 0 & -\sin \phi & \cos \phi \end{bmatrix} \begin{bmatrix} \cos \theta & 0 & -\sin \theta \\ 0 & 1 & 0 \\ \sin \theta & 0 & \cos \theta \end{bmatrix} \begin{bmatrix} \cos \psi & \sin \psi & 0 \\ -\sin \psi & \cos \psi & 0 \\ 0 & 0 & 1 \end{bmatrix}}_{R_0^1} \begin{bmatrix} x_0 \\ y_0 \\ z_0 \end{bmatrix} \quad (53.7)$$

$$R_0^1 = \begin{bmatrix} \cos \theta \cos \psi & \cos \theta \sin \psi & -\sin \theta \\ -\cos \theta \sin \psi + \sin \phi \sin \theta \cos \psi & \cos \phi \cos \psi + \sin \phi \sin \theta \sin \psi & \sin \phi \cos \theta \\ \sin \phi \sin \psi + \cos \phi \sin \theta \cos \psi & -\sin \phi \cos \psi + \cos \phi \sin \theta \sin \psi & \cos \phi \cos \theta \end{bmatrix} \quad (53.8)$$

This matrix, which represents a transformation resulting from three sequential Euler angle rotations, will be used throughout the chapter.

Overall, any rotation matrix has a number of properties. They are summarized here for completeness; an interested reader is referred to references (Goldstein 1980; Murray et al. 1994) for thorough details:

- Rotation matrices are orthogonal.
- The determinant of a rotation matrix is unity.
- Successive rotations can be represented by the ordered product of the individual rotation matrices.
- Rotation matrices are not commutative; hence, in general case,  $R_b^c R_a^b \neq R_a^b R_b^c$ .
- A nontrivial rotation matrix has only one eigenvalue equal to unity with other two, being a complex conjugate pair with unity magnitude; a trivial rotation is described by an identity matrix.

The time rate of change of the DCM matrix that defines the dynamics of the attitude states is important in derivation of the kinematic equations of motion. As it will be shown shortly, it enables relating the sensor (e.g., given by the rate gyros) measurements obtained in a body-fixed frame to the time derivatives of the Euler angles describing the attitude of a body in an inertial frame.

In general case, the time derivative of a rotation matrix that is considered as a function of time can be obtained based on its key properties. Let  $R(t) = R_0^1(t)$  be a rotation matrix given as a function of time. Since  $R \cdot R^T = I$ , taking the time derivative of both sides yields

$$\frac{d(R \cdot R^T)}{dt} = \dot{R} \cdot R^T + R \cdot \dot{R}^T = \dot{R} \cdot R^T + (\dot{R} \cdot R^T)^T = \mathbf{0}.$$

First, it can be observed that  $\dot{R} \cdot R^T = S$  is a skew symmetric matrix. Next, let  $\mathbf{p}_1 = R(t)\mathbf{p}_0$ , where  $\mathbf{p}_0$  is a vector of constant length rotated over time with an angular velocity vector  $\Omega$ . Comparing two expressions of the absolute time derivatives of  $\mathbf{p}_1$

$$\dot{\mathbf{p}}_1 = \dot{R}(t)\mathbf{p}_0 = S(t)R(t) \cdot \mathbf{p}_0 = S(t) \cdot \mathbf{p}_1,$$

$$\dot{\mathbf{p}}_1 = \Omega \times \mathbf{p}_1 = S(\Omega(t)) \cdot \mathbf{p}_1$$

217 leads to

$$218 \quad \dot{R} = S(\Omega)R, \quad S(\Omega) = \dot{R}R^T. \quad (53.9)$$

219 Thus, the skew symmetric matrix  $S(\Omega)$  in (53.9) is used to represent the vector  
220 cross product between the vectors  $\Omega$  and the  $R(t)\mathbf{p}_0$ . The matrix  $S(\Omega)$ , where vector  
221  $\Omega = [\omega_x, \omega_y, \omega_z]^T$  is represented by its components, can be written in the form

$$222 \quad S(\Omega) = \begin{bmatrix} 0 & \omega_z & -\omega_y \\ -\omega_z & 0 & \omega_x \\ \omega_y & -\omega_x & 0 \end{bmatrix}.$$

223 Another useful general property of angular velocities is called the *angular velocities*  
224 *addition theorem* (Rogers 2003). The theorem states that for angular velocity vectors  
225 coordinated in a common frame, the resulting angular velocity of the cumulative  
226 rotation is a plain sum of the contributing rotations. Now, if a rotating frame is given  
227 by a set of time varying Euler angles  $[\psi, \theta, \phi]$  defined with respect to a stationary  
228 frame, then it is straightforward to determine the components of the angular velocity  
229 vector  $\Omega = [\omega_x, \omega_y, \omega_z]^T$  as though measured in the rotating frame. Starting from  
230 an initial stationary frame (see Fig. 53.2) and using two intermediate frames whose  
231 relative angular velocities are defined by the Euler angle rates  $[\dot{\psi}, \dot{\theta}, \dot{\phi}]$  and utilizing  
232 the angular velocities addition theorem, the following kinematic equation can be  
233 obtained:

$$234 \quad \begin{bmatrix} \omega_x \\ \omega_y \\ \omega_z \end{bmatrix} = R_\phi R_\theta \begin{bmatrix} 0 \\ 0 \\ \dot{\psi} \end{bmatrix} + R_\phi \begin{bmatrix} 0 \\ \dot{\theta} \\ 0 \end{bmatrix} + \begin{bmatrix} \dot{\phi} \\ 0 \\ 0 \end{bmatrix} \quad (53.10)$$

235 Substituting the corresponding DCM matrices from (53.7) results in

$$236 \quad \begin{bmatrix} \omega_x \\ \omega_y \\ \omega_z \end{bmatrix} = \begin{bmatrix} 1 & 0 & -\sin \theta \\ 0 & \cos \phi & \cos \theta \sin \phi \\ 0 & -\sin \phi & \cos \theta \cos \phi \end{bmatrix} \begin{bmatrix} \dot{\phi} \\ \dot{\theta} \\ \dot{\psi} \end{bmatrix} \quad (53.11)$$

237 Inverting the last equation results in equation

$$238 \quad \begin{bmatrix} \dot{\phi} \\ \dot{\theta} \\ \dot{\psi} \end{bmatrix} = \begin{bmatrix} 1 & \sin \phi \frac{\sin \theta}{\cos \theta} & \cos \phi \frac{\sin \theta}{\cos \theta} \\ 0 & \cos \phi & -\sin \phi \\ 0 & \sin \phi \frac{1}{\cos \theta} & \cos \phi \frac{1}{\cos \theta} \end{bmatrix} \begin{bmatrix} \omega_x \\ \omega_y \\ \omega_z \end{bmatrix} \quad (53.12)$$

239 that defines the derivatives of the Euler angles in terms of the angles themselves  
240 and the angular velocity vector  $\Omega = [\omega_x, \omega_y, \omega_z]^T$  as it was measured in the  
241 rotated frame. These equations define the rotational kinematics of a rigid body; they  
242 contribute to the final set of 6DoF equations of motion.

243 Analysis of the (53.12) shows that four elements of the inverted matrix become  
244 singular when the second rotation angle  $\theta$  approaches  $\pi/2$ . This problem is usually  
245 called a *kinematic singularity* or a *gimbal lock* in navigation and is one of the

issues associated with the use of Euler angles for the attitude determination. For differently ordered Euler rotation sequences, the kinematic singularity will occur at a different point. Therefore, one way to avoid the singularity is to switch or change the Euler angle sequences when approaching the singularity. Next, depending on the available computing power, the integration of the kinematic equation (53.12) can be computationally expensive because it involves calculation of trigonometric functions. Furthermore, it can be observed that the Euler angle-based DCM matrix is redundant; it requires only 3 out of 9 elements of the DCM matrix to uniquely define the Euler angles. These shortcomings usually result in applying different parameters describing the attitude and its dynamic transformation.

In applications to the fixed-wing UAV attitude determination, the Rodrigues–Hamilton parameter, or quaternion, is one of the most widely used alternatives (Goldstein 1980). Utilizing the quaternion approach is very powerful because it gives a singularity-free attitude determination at any orientation of a rigid body. Next, since it can be shown that the equations of motion of a rigid body are linear differential equations in the components of quaternion, then it (linearity) is a desirable property, especially when developing estimation and control algorithms. Furthermore, the quaternion is a relatively computationally efficient approach since it does not involve trigonometric functions to compute the attitude matrix and has only one redundant parameter, as opposed to the six redundant elements of the attitude matrix. However, it is also worth noting that the quaternion and Euler angle techniques are both widely used in various UAV applications; the equations connecting both representations are well developed, thus enabling complementary definition of the DCM matrix and Euler angles through the parameters of quaternion and vice versa. An interested reader is referred to an extensive historical survey of attitude representations (Shuster 1993) and references (Rogers 2003; Goldstein 1980; Murray et al. 1994) for more details in the alternative methods of attitude determination.

AU4

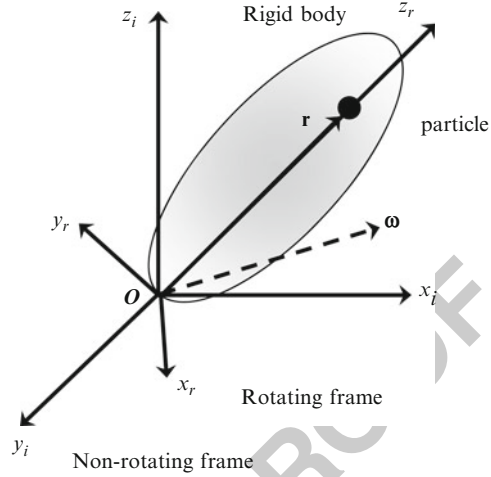
### 53.2.2 Generalized Motion

In the development of dynamic equations of motion, it will be necessary to calculate the absolute time derivative of a vector defined in coordinate frames that rotate and move with respect to each other. In an application to the UAV kinematics, this can be justified by a necessity to relate the absolute time derivative of a position vector in inertial space (inertial velocity) that is defined based on the measurements taken in a body frame. Similarly, the second time derivative defines the body inertial acceleration.

Consider two coordinate frames  $\{F_i\}$  and  $\{F_r\}$ , where  $i$  stands for an inertial not rotating frame and  $r$  stands for the rotating frame. The first objective is to calculate the derivative of a unity vector  $\mathbf{r}_r$  defined in  $\{F_r\}$  attached to a rigid body rotating with respect to the  $\{F_i\}$  with angular speed  $\boldsymbol{\omega}$ ; see Fig. 53.3. Denote the rotation from  $\{F_r\}$  to  $\{F_i\}$  as  $R$ :

$$\mathbf{r}_i = R\mathbf{r}_r$$

**Fig. 53.3** Deriving the time derivative of a vector



288 Taking the derivative results in

$$289 \quad \dot{\mathbf{r}}_i = \dot{R}\mathbf{r}_r + R\dot{\mathbf{r}}_r = \dot{R}\mathbf{r}_r = S(\boldsymbol{\omega})\mathbf{r}_r = \boldsymbol{\omega} \times \mathbf{r}_r, \quad (53.13)$$

291 where the time derivative  $\dot{\mathbf{r}}_r$  is zero due to the rigid body assumption.

292 Next, using the same setup, calculate the absolute time derivative of an arbitrary  
293 time varying vector  $\mathbf{r}$  defined in  $\{F_r\}$ . Defining the vector in terms of its components  
294 in both frames and taking its time derivative in the inertial frame result in

$$295 \quad \mathbf{r} = r_{xi}\mathbf{i} + r_{yi}\mathbf{j} + r_{zi}\mathbf{k} = r_{xr}\mathbf{l} + r_{yr}\mathbf{m} + r_{zr}\mathbf{n}.$$

296 Taking the absolute time derivative of both expressions gives

$$297 \quad \begin{aligned} \frac{d\mathbf{r}}{dt} &= \dot{r}_{xi}\mathbf{i} + \dot{r}_{yi}\mathbf{j} + \dot{r}_{zi}\mathbf{k} \\ \frac{d\mathbf{r}}{dt} &= \dot{r}_{xr}\mathbf{l} + \dot{r}_{yr}\mathbf{m} + \dot{r}_{zr}\mathbf{n} + r_{xr}\dot{\mathbf{l}} + r_{yr}\dot{\mathbf{m}} + r_{zr}\dot{\mathbf{n}}. \end{aligned}$$

298 Applying (53.13) allows rewriting the last equation as

$$299 \quad \frac{d\mathbf{r}}{dt} = \frac{\delta\mathbf{r}}{\delta t} + \boldsymbol{\omega} \times \mathbf{r} = \dot{\mathbf{r}}_r + \boldsymbol{\omega} \times \mathbf{r}, \quad (53.14)$$

300 which expresses the derivative of the vector  $\mathbf{r}$  in the inertial frame  $\{F_i\}$  in terms of  
301 its change ( $\dot{\mathbf{r}}_r$ ) calculated in a rotating frame  $\{F_r\}$  and its relative rotation defined by  
302 the angular velocity  $\boldsymbol{\omega}$ . The result in (53.14) is known as the *Coriolis theorem*. The  
303 second derivative of  $\mathbf{r}$  defines the body acceleration and is used in the development  
304 of the dynamic equations. It is obtained in a similar manner by recursively applying  
305 the Coriolis theorem, thus leading to

$$\begin{aligned}
 306 \quad \ddot{\mathbf{r}} &= \frac{\delta}{\delta t}(\dot{\mathbf{r}}_r + \boldsymbol{\omega} \times \mathbf{r}) + \boldsymbol{\omega} \times (\dot{\mathbf{r}}_r + \boldsymbol{\omega} \times \mathbf{r}) \\
 307 \quad &= \ddot{\mathbf{r}}_r + \frac{\delta \boldsymbol{\omega}}{\delta t} \times \mathbf{r} + \boldsymbol{\omega} \times \frac{\delta \mathbf{r}}{\delta t} + \boldsymbol{\omega} \times \dot{\mathbf{r}}_r + \boldsymbol{\omega} \times (\boldsymbol{\omega} \times \mathbf{r}), \\
 308 \quad \ddot{\mathbf{r}} &= \ddot{\mathbf{r}}_r + \dot{\boldsymbol{\omega}} \times \mathbf{r} + 2\boldsymbol{\omega} \times \dot{\mathbf{r}}_r + \boldsymbol{\omega} \times (\boldsymbol{\omega} \times \mathbf{r}). \quad (53.15)
 \end{aligned}$$

309 Similarly to (53.14) where  $\dot{\mathbf{r}}_r$  denotes the local derivative taken in a rotating frame  
 310  $\{F_r\}$ , the  $\frac{\delta \boldsymbol{\omega}}{\delta t}$  refers to the derivative of angular velocity  $\boldsymbol{\omega}$  taken in  $\{F_r\}$  frame.  
 311 However, it can be easily demonstrated

$$312 \quad \frac{d\boldsymbol{\omega}}{dt} = \frac{\delta \boldsymbol{\omega}}{\delta t} + \boldsymbol{\omega} \times \boldsymbol{\omega} = \frac{\delta \boldsymbol{\omega}}{\delta t} \quad (53.16)$$

313 that the derivative of  $\boldsymbol{\omega}$  is independent on the coordinate frame. In turn, this justifies  
 314 omitting the subscript in  $\boldsymbol{\omega}$  referring to  $\{F_r\}$ . The last two terms in (53.15) are  
 315 commonly known as *Coriolis* and the *centripetal accelerations* correspondingly.  
 316 The following chapter heavily relies on the results in (53.14) and (53.15) when it  
 317 develops the dynamic equations of motion.

### 318 53.2.3 Coordinate Frames

319 Deriving equations of motion of a fixed-wing UAV requires a definition of coordi-  
 320 nate frames where forces and moments acting on the airplane can be conveniently  
 321 defined and where the states including the position, velocity, acceleration, and  
 322 attitude can be suitably described. It is worth noting that with the latest advances  
 323 in power technologies and novel materials, a mission of long duration becomes a  
 324 reality. As an example, solar power technology is one of the alternatives that can  
 325 make the 24/7 flight of a fixed-wing solar powered autonomous soaring gliders  
 326 feasible. Thus, the long duration and great operational distances might require  
 327 considering the UAV flight operations with respect to the rotating Earth. This  
 328 consideration would extend the set of coordinate frames used in long-endurance  
 329 UAV applications. The primary reason for such an extension would lie in the  
 330 necessity to resolve the inertial angular velocity of rotation of a body frame in  
 331 a “true” inertial frame where the Earth rotation can be resolved. Those frames  
 332 would include the Earth-centered inertial, Earth-centered Earth-fixed, and a geodetic  
 333 coordinate frames. Consequently, the angular velocities addition theorem mention  
 334 above would be used to resolve the angular velocity vector of body rotation with  
 335 respect to the inertial frame as a vector sum of angular velocities of the intermediate  
 336 frames. An interested reader is referred to (Rogers 2003) for more details in the  
 337 coordinate frames and transformations used in inertial navigation.

338 Therefore, in addition to the body and wind frames that define dynamics of the  
 339 body–fluid interaction, this subsection defines the following set of coordinate frames  
 340 used in various UAV applications:

- 341 1. Earth-centered inertial frame  $\{i\}$
- 342 2. Earth-centered Earth-fixed frame  $\{e\}$

- 343 3. Geodetic coordinate system  $\{\lambda, \varphi, h\}$
- 344 4. Tangent plane coordinate system  $\{u\}$
- 345 5. Body-carried frame  $\{n\}$
- 346 6. Body-fixed frame  $\{b\}$
- 347 7. Wind frame  $\{w\}$

AU5

348 Depending on the duration of flight and operational range, both dictated by a  
 349 specific UAV application, the first four frames can be considered inertial frames,  
 350 with the remaining three frames body fixed. The positioning of inertial and body  
 351 frames is related by a plain translation, while the orientation of body frames relates  
 352 to each other by pure rotations. Details of the frame definition and their relations are  
 353 the subject of this section.

### 354 53.2.3.1 Earth-Centered and Geodetic Coordinate Frames

AU6

355 It is convenient to consider two coordinate frames connected to the Earth. The  
 356 *Earth-centered Earth-fixed* (ECEF) coordinate system is fixed to the Earth, and  
 357 therefore, it rotates at the Earth's sidereal rate with respect to the *Earth-centered*  
 358 *inertial* (ECI) frame that represents nonrotating inertial frame. The ECI frame is  
 359 usually denoted  $\{i\}$  while the ECEF frame is denoted  $\{e\}$ . Both frames are right-  
 360 handed orthogonal and have their origins at the center of the Earth. The ECI frame  
 361 has its  $z_i$  axis aligned with the direction of the Earth's rotation vector and  $x_i$  and  
 362  $y_i$  axes placed in the equatorial plane with  $x_i$  fixed in some celestial reference  
 363 direction, for example, a line connecting the Sun's center and the Earth's position at  
 364 vernal equinox (Kaplan 1981). The ECEF has  $x_e$  and  $y_e$  axes placed in the equatorial  
 365 plane and  $z_e$  axis aligned with  $z_i$  axis; see Fig. 53.4 where the Earth is modeled as  
 366 a spheroid. The  $x_e$  axis is usually attached to the intersection of the Greenwich  
 367 meridian and the equator, and the  $y_e$  axis completes the right-hand system.

368 It is worth noting that the ECEF axes definition may vary; however, the definition  
 369 always states the attachment of two vectors to the direction of the Earth rotation  
 370 and the Greenwich meridian as the inherent Earth properties. The sidereal rate  
 371  $\Omega_i^e$  is the vector defining the ECEF rotation with respect to the ECI; the latter  
 372 one is often called the true inertial frame. If necessary, for the purpose of UAV  
 373 flight description, the magnitude  $\Omega_i^e$  of the rate can be approximated by one full  
 374 rotation in 23h56'4.099", thus resulting in  $\Omega_i^e = 15.04106718$  deg/h. Therefore,  
 375 the transformation from ECI to ECEF frame is a plain rotation around the  $z_i$  axis  
 376 defined by a single rotation by an angle  $\Omega_i^e \cdot t$ , where  $t$  is the time interval.

377 The *local geodetic*  $\{\lambda, \varphi, h\}$  frame is usually associated with the ECEF frame,  
 378 see Fig. 53.4. It has the same origin placed at the center of the Earth. The frame  
 379 defines the orientation of a line normal to Earth's surface and passing through  
 380 the point of interest. The orientation of the line is defined by two angles,  $\lambda$   
 381 (geodetic longitude) and  $\varphi$  (geodetic latitude), with the height  $h$  above the Earth's  
 382 surface; eventually these three parameters, along with the components of the UAV  
 383 velocity vector, become the major navigation states. For most UAV applications, it  
 384 is sufficiently accurate to model Earth's surface as an oblate spheroid with given  $r_e$   
 385 (equatorial) and  $r_p$  (polar radiuses) or one of the radiuses and the  $e$  (ellipticity)  
 386 (Kaplan 1981). Last revisited in 2004, the datum of World Geodetic System

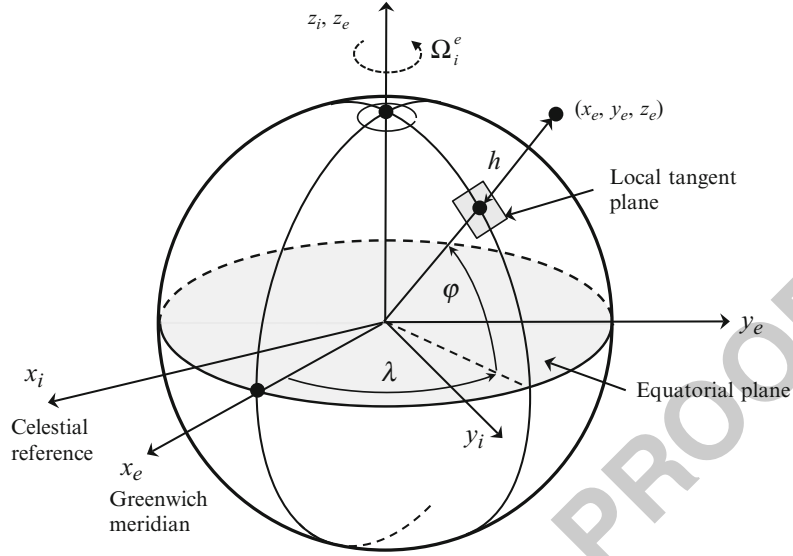


**Fig. 53.4** ECI, ECEF, and geodetic coordinate frames

387 (WGS-84) provides the following parameters for the oblate spheroid modeling:  
 388  $r_e = 6,378,137.00$  m,  $r_p = 6,356,752.314$  m. The resulting transformation from  
 389 the geodetic  $\{\lambda, \varphi, h\}$  to the ECEF frame is as follows:

$$\begin{aligned} x_e &= (r_\lambda + h) \cos \varphi \cos \lambda \\ y_e &= (r_\lambda + h) \cos \varphi \sin \lambda \\ z_e &= ((1 - \varepsilon^2)r_\lambda + h) \sin \varphi \end{aligned} \quad (53.17)$$

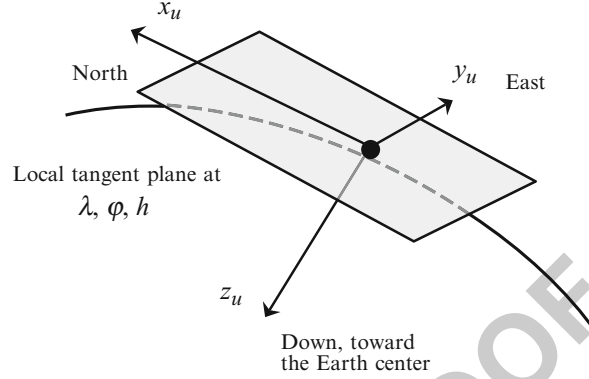
391 where  $\varepsilon$  the eccentricity of oblate ellipsoid is defined as

$$\begin{aligned} r_\lambda &= \frac{r_e}{\sqrt{1 - \varepsilon^2 \sin^2 \varphi}}; \\ \varepsilon &= \sqrt{1 - \frac{r_p^2}{r_e^2}}. \end{aligned}$$

### 394 53.2.3.2 Local Tangent Plane Coordinate System

395 The origin of the *local tangent plane* (LTP) is fixed to the surface of the Earth  
 396 with two of its axes attached to the plane tangent to the surface; see Fig. 53.5.  
 397 The frame is usually marked with the subscript  $\{u\}$  and serves the purpose of an  
 398 inertial frame in most short-duration low-speed UAV applications. The frame's  $x_u$   
 399 and  $y_u$  axes are in the tangent plane and most often aligned with the north and east  
 400 directions correspondingly; the  $z_u$  axis completes the right-hand coordinate system,  
 401 thus pointing down. Quite often the order and alignment of the LTP frame principal

**Fig. 53.5** Definition of the local tangent plane; NED



axes change. In such cases, the LTP coordinate system explicitly specifies its type; in the nominal case presented above, it can be also defined as an NED frame indicating the north–east down alignment of the coordinate axes.

When the origin of the LTP frame is defined in terms of its geodetic latitude, longitude, and altitude above the ground surface, then the equations (53.17) can be applied to define the kinematics of navigation states.

### 53.2.3.3 Body-Carried and Fixed Frames

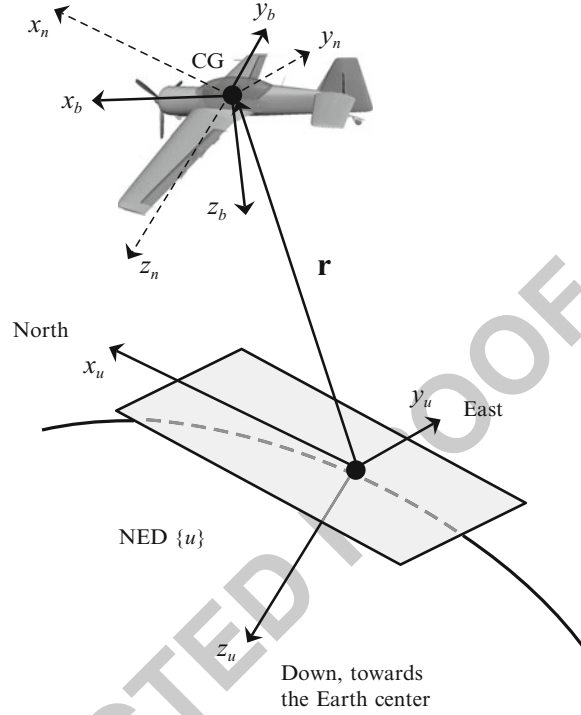
In flight dynamics, the body-attached reference frames usually have their origin at the center of gravity (CG) of an airplane; therefore, these frames are moving. The *body-carried* frame  $\{n\}$  is an orthogonal frame originated at the CG of the UAV. All its axes are permanently stabilized and aligned with the LTP frame axes as it was connected to the CG; see Fig. 53.6; the frame is usually utilized in defining the navigation equations thus assigning its subscript  $\{n\}$ . This frame is connected to the LTP frame by means of a plain translation  $\mathbf{r} = [r_n, r_e, r_d]^T$ .

The *body-fixed* frame is an orthogonal frame defined with respect to the body-carried frame. Its origin is at the CG of UAV, and its axes are rigidly connected to the body; therefore, the frame also rotates with the body. The frame is usually marked with the subscript  $\{b\}$ . The alignment of the  $\{b\}$  frame axes is a degree of freedom that can exploit the body symmetry. It can be proven (Goldstein 1980) that for every rigid body, there is always an orthogonal coordinate system, usually called principal, in which the cross products of inertia terms are zero. Assuming that a typical UAV has at least one plane of symmetry (geometric and mass symmetry) results in two of the body-fixed axes lying in the plane of symmetry. When the axes are aligned along the principal axes of inertia of the body, as will be shown in the following chapter, the dynamic equations of motion become significantly simpler. In a majority of fixed-wing UAV configurations, the axes of  $\{b\}$  frame match the principal axes of inertia. The typical orientation of the body-fixed axes is as follows (see Fig. 53.6): if the UAV has a vertical plane of symmetry, then  $x_b$  and  $z_b$  lie in that plane of symmetry;  $x_b$  points toward the direction of flight and  $z_b$  points downward and  $y_b$  points right, thus completing the right-hand system.

AU7



**Fig. 53.6** Definition of the body-fixed frame with respect to LTP frame



As the body moves, its attitude is defined with reference to the body-carried frame  $\{n\}$  by three consecutive Euler rotations by  $\psi$  (yaw),  $\theta$  (pitch), and  $\phi$  (roll) angles. See their graphical illustration in Fig. 53.2 where frames  $\{0\}$  and  $\{1\}$  relate to the frames  $\{n\}$  and  $\{b\}$  correspondingly. The formal definition of the Euler angles in the application to an airplane attitude specification is presented here for completeness:

- $\psi$  – yaw is the angle between  $x_n$  and the projection of  $x_b$  on the local horizontal plane.
- $\theta$  – pitch is the angle between the local horizon and the  $x_b$  axis measured in the vertical plane of symmetry of the UAV.
- $\phi$  – roll is the angle between the body-fixed  $y_b$  axis and the local horizon measured in the plane  $y_b z_b$ .

As it follows from the attitude representation section, the DCM matrix  $R_u^b$  transforming the body-carried  $\{n\}$  to the body-fixed  $\{b\}$  frame can be constructed as in (53.8). Now the subscripts ( $u \rightarrow b$ ) denote the rotation from the LTP  $\{u\}$  to the body-fixed frame;  $\{u\}$  and  $\{n\}$  frames are always aligned by the definition of body-carried frame.

The application of the rotation matrix (53.8) immediately follows from the need to describe the UAV translational motion in an inertial frame of reference by utilizing the inertial velocity measurements taken in the body-fixed frame at

CG –  $\mathbf{V}_b^g = [u, v, w]^T$ . To this end, consider Fig. 53.6 where vector  $\mathbf{r} = [r_n, r_e, r_d]^T$  denotes the position of an airplane CG with respect to the LTP (NED) frame attached to the Earth. Relating the translational velocity and position and accounting for the fact that *body-carried* frame  $\{n\}$  is stabilized with respect to the nonrotating  $\{u\}$  frame results in

$$\frac{d\mathbf{r}}{dt} = R_b^u \mathbf{V}_b^g$$

$$\frac{d}{dt} \begin{bmatrix} r_n \\ r_e \\ r_d \end{bmatrix} = R_b^u \begin{bmatrix} u \\ v \\ w \end{bmatrix}. \quad (53.18)$$

The relation between the Euler angles defining the relation between the stabilized  $\{n\}$  frame and the body-fixed frame  $\{b\}$  was already derived in (53.11) and (53.12). They define the dynamics of Euler angles defined in an inertial frame with respect to the rates measured in the body-fixed frame. Thus, the kinematic equations (53.12) and (53.18) represent the dynamics of translational and rotational coordinates and therefore are part of the final set of equations of motion.

#### 53.2.3.4 Wind Frame

Aerodynamic forces and moments resulting from the body–air interaction as the airframe moves through the air depend on the body orientation with respect to the surrounding air. In other words, they depend on the vector representing the wind. The velocity vector of the possibly moving air (wind) resolved in the inertial frame  $\{u\}$  is denoted  $\mathbf{V}_u^a$ ; see Fig. 53.7. The magnitude of  $\mathbf{V}_u^a$  is called an *airspeed*  $V_a$ , as opposed to the velocity vector defined in LTP with respect to the ground – *ground speed* vector  $\mathbf{V}_u^g$ . The orientation of the wind frame  $\{w\}$  defined by the direction of  $\mathbf{V}_u^a$  with respect to the body-fixed  $\{b\}$  is defined by two angles.

To generate the lift force in flight, the wing of the UAV must be oriented at a positive angle  $\alpha$  with respect to the  $\mathbf{V}_u^a$  vector. This angle is called the *angle of attack*. The angle of attack  $\alpha$  is also one of the key parameters that define the longitudinal

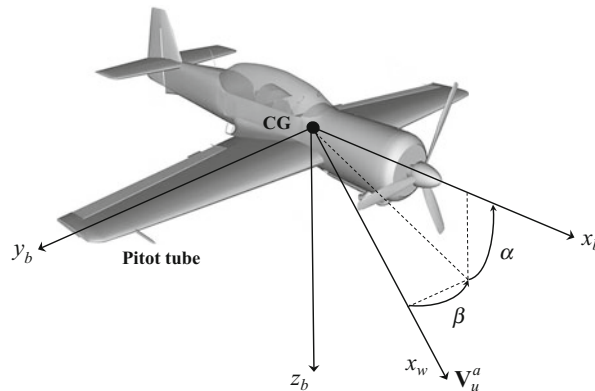


**Fig. 53.7** Wind frame and body-fixed frames. Definition of the angle of attack and the sideslip

476 stability of an airplane. Therefore, quite often, the coordinate frame that results from  
 477 a single rotation from the body-fixed  $\{b\}$  frame on angle  $\alpha$  is called a stability frame  
 478 (Beard and McLain 2012; Etkin and Reid 1995). As illustrated in Fig. 53.7, the angle  
 479 of attack is defined by the projection of  $\mathbf{V}_u^a$  into a vertical plane of symmetry of the  
 480 UAV (spanned by axes  $x_b, z_b$  in frame  $\{b\}$ ) and the longitudinal axis  $x_b$  of the UAV.  
 481 It is positive when a leading edge of the wing rotates upward with respect to the  $\mathbf{V}_u^a$ .  
 482 In turn, the angle between the velocity vector  $\mathbf{V}_u^a$  projected into the “wing-level”  
 483 plane (spanned by axes  $x_b, y_b$  in frame  $\{b\}$ ) and the longitudinal axis  $x_b$  of UAV is  
 484 called the *sideslip angle*. It is denoted by  $\beta$ .

485 Then the transformation from the body-fixed frame  $\{b\}$  to the wind frame  $\{w\}$  is AU8  
 486 given by

$$\begin{aligned}
 487 \quad R_b^w &= \begin{bmatrix} \cos \beta & \sin \beta & 0 \\ -\sin \beta & \cos \beta & 0 \\ 0 & 0 & 1 \end{bmatrix} \begin{bmatrix} \cos \alpha & 0 & \sin \alpha \\ 0 & 1 & 0 \\ -\sin \alpha & 0 & \cos \alpha \end{bmatrix} \\
 488 \quad &= \begin{bmatrix} \cos \alpha \cos \beta & \sin \beta & \sin \alpha \cos \beta \\ -\cos \alpha \sin \beta & \cos \beta & -\sin \alpha \sin \beta \\ -\sin \alpha & 0 & \cos \alpha \end{bmatrix}. \quad (53.19)
 \end{aligned}$$

489 The inverse transformation from the wind frame  $\{w\}$  to the body-fixed frame  $\{b\}$  is  
 490 the transpose of (53.19):  $R_w^b = (R_b^w)^T$ .

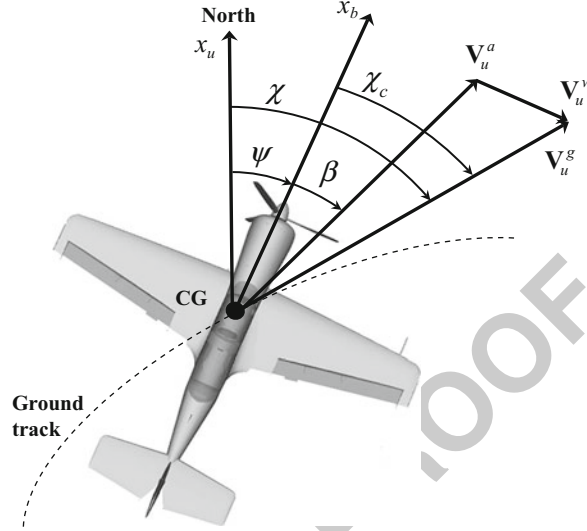
491 The importance of the wind frame in application to the UAVs flying in wind  
 492 conditions that might contribute up to 100 % of the nominal airplane speed cannot  
 493 be overestimated. As an example, imagine an autonomous glider that is designed  
 494 to utilize the wind energy to sustain the long duration of flight. Therefore, it is  
 495 necessary to understand the difference between the airspeed, represented by the air  
 496 velocity vector  $\mathbf{V}_u^a$  and the ground speed  $\mathbf{V}_u^g$ , both resolved with respect to the LTP  
 497 frame. Consider the graphical representation of the relation between these vectors  
 498 in Fig. 53.8. In the presence of constant wind, these velocities are related by the  
 499 equation that is often called the *wind triangle*:

$$500 \quad \mathbf{V}_u^a = \mathbf{V}_u^g - \mathbf{V}_u^w \quad (53.20)$$

501 where  $\mathbf{V}_u^w$  is the wind velocity defined in the LTP frame.

502 The objective of the following development is to define the relations among these  
 503 velocities defined in three different frames, while being measured or estimated by  
 504 the sensors installed in the body-fixed and in the inertial frame. First, define the  
 505 components of all three vectors in the body-fixed frame  $\{b\}$ . Let the UAV velocity  
 506 in the LTP (inertial) frame expressed in the body frame be  $\mathbf{V}_b^g = [u, v, w]^T$ , and let  
 507 the wind velocity in the LTP frame expressed in body frame be  $\mathbf{V}_b^w = [u_w, v_w, w_w]^T$ .  
 508 Observe that  $\mathbf{V}_u^a$  can be expressed in  $\{w\}$  frame as  $\mathbf{V}_w^a = [V_a \ 0 \ 0]^T$ , and let  $\mathbf{V}_b^a =$   
 509  $[u_a \ v_a \ w_a]^T$  be its components expressed in the body frame. Utilizing the definition  
 510 of the angles of attack and sideslip relating the wind frame to the body-fixed frame  
 511 and the “wind triangle” (53.20) expressed in the body frame results in the following:

**Fig. 53.8** Wind triangle in 2D plane and the yaw ( $\psi$ ), sideslip ( $\beta$ ), and course ( $\chi$ ) angles



$$\begin{aligned}
 \mathbf{V}_b^a &= \mathbf{V}_b^g - \mathbf{V}_b^w = \begin{bmatrix} u \\ v \\ w \end{bmatrix} - \begin{bmatrix} u_w \\ v_w \\ w_w \end{bmatrix} \\
 \mathbf{V}_b^a &= \begin{bmatrix} u_a \\ v_a \\ w_a \end{bmatrix} = R_w^b \begin{bmatrix} V_a \\ 0 \\ 0 \end{bmatrix} = \begin{bmatrix} \cos \alpha \cos \beta & \sin \beta & \sin \alpha \cos \beta \\ -\cos \alpha \sin \beta & \cos \beta & -\sin \alpha \sin \beta \\ -\sin \alpha & 0 & \cos \alpha \end{bmatrix} \begin{bmatrix} V_a \\ 0 \\ 0 \end{bmatrix} \\
 \begin{bmatrix} u_a \\ v_a \\ w_a \end{bmatrix} &= V_a \begin{bmatrix} \cos \alpha \cos \beta \\ \sin \beta \\ \sin \alpha \cos \beta \end{bmatrix} \tag{53.21}
 \end{aligned}$$

This last equation relates the airspeed components of  $\mathbf{V}_b^a$  resolved in the body frame with the airspeed and the angles of attack and sideslip. In turn, if the wind components resolved in the body frame are known, then inverting the last equation allows for calculation of the airspeed  $V_a$  and the  $\alpha, \beta$  angles:

$$V_a = \sqrt{u_a^2 + v_a^2 + w_a^2}, \quad \alpha = \arctan\left(\frac{w_a}{u_a}\right), \quad \beta = \arcsin\left(\frac{v_a}{V_a}\right). \tag{53.22}$$

### 53.2.3.5 Summary of Kinematics

This section developed the fundamental kinematic equations that not only define the kinematics of states and contribute to the final set of 6DoF equations of motion but also serve as the basis for the design of the guidance and navigation tasks. There are numerous publications describing the kinematics of moving frames. Most of the publications originate in the area of classical mechanics and rigid body

526 dynamics (Murray et al. 1994; Goldstein 1980). The publications in the area of flight  
527 dynamics and control always contain material addressing the attitude representation  
528 techniques and differential rotations and thus can be a good source of reference  
529 information. The most recent and thorough presentation of these topics can be found  
530 in (Beard and McLain 2012) where the authors specifically address the kinematics  
531 and dynamics of small UAVs.

### 532 53.3 Rigid Body Dynamics

533 This section addresses the development of the dynamics of a rigid body. The  
534 discussion is based on the application of the Newton’s laws in the cases of linear  
535 and angular motion. In particular, the Newton’s second law of motion states that the  
536 sum of all external forces acting on a body in an inertial frame must be equal to  
537 the time rate of change of its linear momentum. On the other hand, the sum of the  
538 external moments acting on a body must be equal to the time rate of change of its  
539 angular momentum. The application of these laws is the objective of this chapter.

540 Thus, a fixed-wing UAV is considered as the rigid body, and its dynamics is  
541 defined with respect to the body-fixed coordinate system. The approach considers  
542 a typical fixed-wing UAV operating in a small region of the Earth thus justifying  
543 the assumption of LTP frame as an inertial frame. Relations necessary to translate  
544 the inertial forces to the body-fixed frame are also presented. Before proceeding to  
545 the derivation, it is necessary to present some assumptions typical for the fixed-wing  
546 UAVs:

547 **A1.** The mass of the UAV remains constant during flight.

548 **A2.** The UAV is a rigid body.

549 The relations derived in this chapter are general and can be applied to any rigid  
550 body; however, the treatment of the aerodynamic forces and moments acting on the  
551 body will be specific to the aerodynamically controlled fixed-wing UAVs.

#### 552 53.3.1 Conservation of Linear Momentum

553 First, assume that a rigid body consists of a set of  $i$  “isolated” elementary particles  
554 with mass  $m_i$  exposed to the external force  $\mathbf{F}_u^i$  while being connected together by  
555 the internal forces  $\mathbf{R}_u^i$ . Since the set of  $N$  particles comprises a rigid body structure  
556 (see **A2**), the net force exerted by all the particles is  $\sum_i^N \mathbf{R}_u^i = 0$ . The set of  
557 external forces acting on the body is a combination of the gravity force acting in an  
558 inertial frame  $\{u\}$  and the aerodynamic and propulsion forces defined with respect  
559 to the body-fixed frame  $\{b\}$  but expressed in the inertial frame  $\{u\}$ . Thus, the linear  
560 momentum of a single particle expressed in an inertial frame obeys the equality

$$561 \quad \mathbf{F}_u^i + \mathbf{R}_u^i = \frac{d}{dt}(m_i \mathbf{V}_u^i), \quad (53.23)$$

562 where the time derivative is taken in an inertial frame. Summing up all the  $N$  parti-  
563 cles comprising the body gives the linear momentum equation of the entire body

$$564 \quad \sum_{i=1}^N \mathbf{F}_u^i = \sum_{i=1}^N \frac{d}{dt} (m_i \mathbf{V}_u^i). \quad (53.24)$$

565 The left-hand side of this equation represents the sum of all forces (gravitational,  
566 propulsion, and aerodynamic) expressed in an inertial frame, with the right side  
567 depending on the velocity of the body defined in an inertial frame. First, observe  
568 that the individual inertial velocities  $\mathbf{V}_u^i$  are not independent. Since they comprise  
569 a rigid body, their vectors can be represented as a sum of  $\mathbf{V}_b^g$  the inertial velocity  
570 vector resolved in  $\{b\}$  frame with respect to CG plus the velocity vector induced by  
571 the body rotation with respect to the CG and defined by the radius vector  $\mathbf{r}_b^i$  of the  
572  $i$ th particle in  $\{b\}$  frame; thus  $\mathbf{V}_u^i = \mathbf{V}_b^g + \boldsymbol{\omega} \times \mathbf{r}_b^i$ . Next, using an assumption **A1** and  
573 utilizing the result in (53.14) for the total velocity of the  $i$ th particle in an inertial  
574 frame, allows for the calculation of the absolute time derivatives in an inertial frame  
575 in the following form:

$$\begin{aligned} 576 \quad \sum_{i=1}^N \mathbf{F}_u^i &= \sum_{i=1}^N \frac{d}{dt} (m_i \mathbf{V}_u^i) = \sum_{i=1}^N \frac{d}{dt} (m_i (\mathbf{V}_b^g + \boldsymbol{\omega} \times \mathbf{r}_b^i)) \\ 577 \quad &= \sum_{i=1}^N m_i \frac{d\mathbf{V}_b^g}{dt} + \sum_{i=1}^N m_i \frac{d}{dt} (\boldsymbol{\omega} \times \mathbf{r}_b^i) \\ 578 \quad &= \sum_{i=1}^N m_i \frac{d\mathbf{V}_b^g}{dt} + \frac{d}{dt} \left[ \boldsymbol{\omega} \times \sum_{i=1}^N m_i \mathbf{r}_b^i \right]. \end{aligned} \quad (53.25)$$

579 Here  $\boldsymbol{\omega}$  represents the angular velocity of the UAV body resolved in the inertial  
580 frame; see (53.14). Defining  $\mathbf{r}_b^{cg}$  the vector of CG location in  $\{b\}$  frame as  $m\mathbf{r}_b^{cg} =$   
581  $\sum_{i=1}^N m_i \mathbf{r}_b^i$ , where  $m = \sum_{i=1}^N m_i$  is the total mass of the body, simplifies the linear  
582 momentum equation:

$$583 \quad \sum_{i=1}^N \mathbf{F}_u^i = m \frac{d\mathbf{V}_b^g}{dt} + m \frac{d}{dt} [\boldsymbol{\omega} \times \mathbf{r}_b^{cg}].$$

584 Resolving all external forces in  $\{b\}$  frame and assuming that the location of CG does  
585 not change with time and applying the result in (53.14) to the absolute derivatives  
586 of the vectors  $\mathbf{V}_b^g$  and  $\boldsymbol{\omega}$  result in

$$587 \quad \mathbf{F}_b = m(\dot{\mathbf{V}}_b^g + \dot{\boldsymbol{\omega}} \times \mathbf{r}_b^{cg} + \boldsymbol{\omega} \times \mathbf{V}_b^g + \boldsymbol{\omega} \times [\boldsymbol{\omega} \times \mathbf{r}_b^{cg}]), \quad (53.26)$$

588 where the vector quantities can be represented in the following scalar form:

589  $\mathbf{F}_b = [X, Y, Z]^T$  – the externally applied forces expressed in the body frame  
 590  $\mathbf{V}_b^g = [u, v, w]^T$  – the inertial velocity components defined in the body frame  
 591  $\boldsymbol{\omega} = [p, q, r]^T$  – the inertial angular velocity resolved in the body frame  
 592  $\mathbf{r}_b^{cg} = [x_{cg}, y_{cg}, z_{cg}]^T$  – the body referenced location of the center of gravity

593 The translation of the inertial forces to the body frame is justified by the  
 594 convenience of calculating the local body frame derivatives of the  $\mathbf{V}_b^g$  and  $\boldsymbol{\omega}$   
 595 expressed in the body frame; the first one results in  $\dot{\mathbf{V}}_b^g$ , while the derivative of  
 596  $\boldsymbol{\omega}$  is independent on the coordinate frame; see (53.16).

597 Utilizing the double vector product identity  $\boldsymbol{\omega} \times [\boldsymbol{\omega} \times \mathbf{r}_b^{cg}] = (\boldsymbol{\omega} \cdot \mathbf{r}_b^{cg}) \cdot \boldsymbol{\omega} -$   
 598  $(\boldsymbol{\omega} \cdot \boldsymbol{\omega}) \cdot \mathbf{r}_b^{cg}$  allows for the expansion of the linear momentum equation in the scalar  
 599 form as follows:

$$\begin{aligned} 600 \quad X &= m [\dot{u} + qw - rv + \dot{z}_{cg} - \dot{y}_{cg} + (qy_{cg} + rz_{cg})p - (q^2 + r^2)x_{cg}] \\ 601 \quad Y &= m [\dot{v} + ru - pw + \dot{x}_{cg} - \dot{z}_{cg} + (rz_{cg} + px_{cg})q - (r^2 + p^2)y_{cg}] \\ 602 \quad Z &= m [\dot{w} + pv - qu + \dot{y}_{cg} - \dot{x}_{cg} + (px_{cg} + qy_{cg})r - (p^2 + q^2)z_{cg}]. \\ 603 \end{aligned} \quad (53.27)$$

604 The last set of equations allows for an arbitrary choice of the body frame origin  $\{b\}$   
 605 with respect to the CG. However, if the origin of the body-fixed frame  $\{b\}$  is chosen  
 606 at the CG, the last set of equations can be significantly simplified by substituting  
 607  $\mathbf{r}_b^{cg} = [0, 0, 0]^T$ , thus leading to

$$608 \quad \mathbf{F}_b = m (\dot{\mathbf{V}}_b^g + \boldsymbol{\omega} \times \mathbf{V}_b^g). \quad (53.28)$$

609 Expanding the cross product results in the following simplified form of the linear  
 610 momentum equation:

$$\begin{aligned} &X = m [\dot{u} + qw - rv] \\ &Y = m [\dot{v} + ru - pw] \\ 611 \quad &Z = m [\dot{w} + pv - qu]. \end{aligned} \quad (53.29)$$

612 Resolving equations (53.29) with respect to the derivatives (accelerations in the body  
 613 frame) leads to the standard form of differential equations suitable for immediate  
 614 mathematical modeling:

$$\begin{aligned} &\dot{u} = \frac{X}{m} + [rv - qw] \\ &\dot{v} = \frac{Y}{m} + [pw - ru] \\ 615 \quad &\dot{w} = \frac{Z}{m} + [qu - pv]. \end{aligned} \quad (53.30)$$

### 53.3.2 Conservation of Angular Momentum

Applying the law of conservation of angular momentum to an  $i$ th particle in a moving frame is very similar to the approach used above. Consider an  $i$ th particle subjected to the internal ( $\mathbf{M}_u^i$ ) and external ( $\mathbf{r}_u^i \times \mathbf{F}_u^i$ ) moments acting on the body in inertial frame. Similar to the linear momentum case, the sum of internal moments acting on the particle of a rigid body (A2) should be equal to zero ( $\sum_{i=1}^N \mathbf{M}_u^i = 0$ ), while the external moments arise from the inertial gravity and the body-attached forces, such as aerodynamic and propulsion. Thus, the conservation of angular momentum calculated across the entire rigid body results in

$$\sum_{i=1}^N (\mathbf{M}_u^i + \mathbf{r}_b^i \times \mathbf{F}_u^i) = \sum_{i=1}^N \mathbf{M}_u^i + \sum_{i=1}^N \mathbf{r}_b^i \times \mathbf{F}_u^i = \sum_{i=1}^N \mathbf{r}_b^i \times \frac{d}{dt}(m_i \mathbf{V}_u^i), \quad (53.31)$$

where the sum of internal moments cancel each other out. Then, applying the Coriolis theorem (53.14) leads to

$$\begin{aligned} \sum_{i=1}^N \mathbf{r}_b^i \times \frac{d}{dt}(m_i \mathbf{V}_u^i) &= \sum_{i=1}^N m_i \mathbf{r}_b^i \times \frac{d}{dt}(\mathbf{V}_u^i) \\ &= \sum_{i=1}^N m_i \mathbf{r}_b^i \times \left( \frac{\delta \mathbf{V}_b^g}{\delta t} + \boldsymbol{\omega} \times \mathbf{V}_b^g + \frac{\delta \boldsymbol{\omega}}{\delta t} \times \mathbf{r}_b^i + \boldsymbol{\omega} \times [\boldsymbol{\omega} \times \mathbf{r}_b^i] \right) \\ &= \sum_{i=1}^N m_i \mathbf{r}_b^i \times \left( \frac{\delta \mathbf{V}_b^g}{\delta t} + \boldsymbol{\omega} \times \mathbf{V}_b^g \right) + \sum_{i=1}^N m_i \mathbf{r}_b^i \times \left[ \frac{\delta \boldsymbol{\omega}}{\delta t} \times \mathbf{r}_b^i \right] \\ &\quad + \sum_{i=1}^N m_i \mathbf{r}_b^i \times [\boldsymbol{\omega} \times [\boldsymbol{\omega} \times \mathbf{r}_b^i]]. \end{aligned} \quad (53.32)$$

The first term can be expanded by utilizing the definition of the CG:

$$\begin{aligned} \sum_{i=1}^N m_i \mathbf{r}_b^i \times \left( \frac{\delta \mathbf{V}_b^g}{\delta t} + \boldsymbol{\omega} \times \mathbf{V}_b^g \right) \\ = m \mathbf{r}_{cg} \times \left( \frac{\delta \mathbf{V}_b^g}{\delta t} + \boldsymbol{\omega} \times \mathbf{V}_b^g \right) = \begin{bmatrix} m [y_{cg}(\dot{w} + pv - qu) - z_{cg}(\dot{v} + ru - pw)] \\ m [z_{cg}(\dot{u} + qw - rv) - x_{cg}(\dot{w} + pv - qu)] \\ m [x_{cg}(\dot{v} + ru - pw) - y_{cg}(\dot{u} + qw - rv)] \end{bmatrix}. \end{aligned} \quad (53.33)$$



Utilizing the double vector product identity allows for the expansion of the second term as follows:

$$\begin{aligned}
 \sum_{i=1}^N m_i \mathbf{r}_b^i \times \left( \frac{\delta \boldsymbol{\omega}}{\delta t} \times \mathbf{r}_b^i \right) &= \sum_{i=1}^N m_i \left( \frac{\delta \boldsymbol{\omega}}{\delta t} (\mathbf{r}_b^i \cdot \mathbf{r}_b^i) - \mathbf{r}_b^i \left( \frac{\delta \boldsymbol{\omega}}{\delta t} \cdot \mathbf{r}_b^i \right) \right) \\
 &= \begin{bmatrix} \sum_{i=1}^N m_i ((y_i^2 + z_i^2) \dot{p} - (y_i \dot{q} + z_i \dot{r}) x_i) \\ \sum_{i=1}^N m_i ((z_i^2 + x_i^2) \dot{q} - (z_i \dot{r} + x_i \dot{p}) y_i) \\ \sum_{i=1}^N m_i ((x_i^2 + y_i^2) \dot{r} - (x_i \dot{p} + y_i \dot{q}) z_i) \end{bmatrix} = \begin{bmatrix} I_{xx} \dot{p} + I_{xy} \dot{q} + I_{xz} \dot{r} \\ I_{yx} \dot{p} + I_{yy} \dot{q} + I_{yz} \dot{r} \\ I_{zx} \dot{p} + I_{zy} \dot{q} + I_{zz} \dot{r} \end{bmatrix} \\
 &= \begin{bmatrix} I_{xx} & I_{xy} & I_{xz} \\ I_{yx} & I_{yy} & I_{yz} \\ I_{zx} & I_{zy} & I_{zz} \end{bmatrix} \begin{bmatrix} \dot{p} \\ \dot{q} \\ \dot{r} \end{bmatrix} = \mathbf{I} \cdot \dot{\boldsymbol{\omega}}. \tag{53.34}
 \end{aligned}$$

The equation (53.34) is obtained by recognizing the moments of inertia and their symmetrical properties:

$$\begin{aligned}
 I_{xx} &= \sum_{i=1}^N m_i (y_i^2 + z_i^2) & I_{yy} &= \sum_{i=1}^N m_i (z_i^2 + x_i^2) & I_{zz} &= \sum_{i=1}^N m_i (x_i^2 + y_i^2) \\
 I_{xy} &= I_{yx} = - \sum_{i=1}^N m_i x_i y_i & I_{xz} &= I_{zx} = - \sum_{i=1}^N m_i x_i z_i & I_{yz} &= I_{zy} = - \sum_{i=1}^N m_i y_i z_i
 \end{aligned}$$

Combining them into a matrix form defines the inertia tensor  $\mathbf{I}$  that allows the conversion of the entire double vector product into a very compact form as in (53.34). The diagonal terms of  $\mathbf{I}$  are called the moments of inertia. The off-diagonal terms are called the products of inertia; they define the inertia cross coupling. The moments of inertia are directly proportional to the UAV's tendency to resist angular acceleration with respect to a specific axis of rotation. For a body with axes of symmetry, the inertia tensor can be resolved (Goldstein 1980) with zero off-diagonal terms that significantly simplify its form and the final equations of angular momentum.

655 The last term in (53.32) utilizes twice the same double cross product expansion,  
656 thus leading to

$$\begin{aligned}
 & \sum_{i=1}^N m_i \mathbf{r}_b^i \times [\boldsymbol{\omega} \times [\boldsymbol{\omega} \times \mathbf{r}_b^i]] = \sum_{i=1}^N m_i \mathbf{r}_b^i \times ((\boldsymbol{\omega} \cdot \mathbf{r}_b^i) \boldsymbol{\omega} - (\boldsymbol{\omega} \cdot \boldsymbol{\omega}) \mathbf{r}_b^i) \\
 657 \quad & = \begin{bmatrix} I_{yz}(q^2 - r^2) + I_{xz}pq - I_{xy}pr \\ I_{xz}(r^2 - p^2) + I_{xy}rq - I_{yz}pq \\ I_{xy}(p^2 - q^2) + I_{yz}pr - I_{xz}qr \end{bmatrix} + \begin{bmatrix} (I_{zz} - I_{yy})rq \\ (I_{xx} - I_{zz})rp \\ (I_{yy} - I_{xx})qp \end{bmatrix}. \quad (53.35)
 \end{aligned}$$

658 Resolving the total inertial moment acting on the UAV in body frame and denoting  
659 the components as  $\mathbf{M}_b = [L, M, N]^T$  and combining the results in (53.33)–(53.35)  
660 lead to the following complete angular momentum equations in an expanded form:

$$\begin{aligned}
 661 \quad L &= I_{xx}\dot{p} + I_{xy}\dot{q} + I_{xz}\dot{r} \\
 662 \quad &+ I_{yz}(q^2 - r^2) + I_{xz}pq - I_{xy}pr + (I_{zz} - I_{yy})rq \\
 663 \quad &+ m[y_{cg}(\dot{w} + pv - qu) - z_{cg}(\dot{v} + ru - pw)] \\
 664 \quad M &= I_{yx}\dot{p} + I_{yy}\dot{q} + I_{yz}\dot{r} \\
 665 \quad &+ I_{xz}(r^2 - p^2) + I_{xy}rq - I_{yz}pq + (I_{xx} - I_{zz})rp \\
 666 \quad &+ m[z_{cg}(\dot{u} + qw - rv) - x_{cg}(\dot{w} + pv - qu)] \\
 667 \quad N &= I_{zx}\dot{p} + I_{zy}\dot{q} + I_{zz}\dot{r} \\
 668 \quad &+ I_{xy}(p^2 - q^2) + I_{yz}pr - I_{xz}qr + (I_{yy} - I_{xx})qp \\
 669 \quad &+ m[x_{cg}(\dot{v} + ru - pw) - y_{cg}(\dot{u} + qw - rv)].
 \end{aligned} \quad (53.36)$$

670 If the origin of the body-fixed frame  $\{b\}$  is chosen at the CG ( $\mathbf{r}_b^{cg} = [0, 0, 0]^T$ ),  
671 then in the case of a typical UAV with a vertical plane of symmetry spanned by the  
672 body-fixed axes  $x_b, z_b$ , the two pairs of the off-diagonal terms of  $\mathbf{I}$  matrix become  
673 zero, namely,  $I_{xy} = I_{yx} = 0$  and  $I_{yz} = I_{zy} = 0$ . This significantly simplifies the  
674 above equations:

$$\begin{aligned}
 & L = I_{xx}\dot{p} + (I_{zz} - I_{yy})rq + I_{xz}(\dot{r} + pq) \\
 675 \quad & M = I_{yy}\dot{q} + (I_{xx} - I_{zz})rp + I_{xz}(r^2 - p^2) \\
 & N = I_{zz}\dot{r} + (I_{yy} - I_{xx})qp + I_{zx}(\dot{p} - qr). \quad (53.37)
 \end{aligned}$$

676 These equations represent the complete rotational dynamics of a typical fixed-wing  
677 UAV modeled as a rigid body with a longitudinal plane of symmetry.

### 53.3.3 Complete Set of 6DoF Equations of Motion

The final set of 6DoF equations of motion describing the kinematics and dynamics of a generic UAV with a longitudinal plane of symmetry modeled as a rigid body can be summarized as follows:

$$\begin{aligned} X &= m [\dot{u} + qw - rv] \\ Y &= m [\dot{v} + ru - pw] \\ Z &= m [\dot{w} + pv - qu] \end{aligned} \quad (53.38)$$

$$\begin{aligned} L &= I_{xx}\dot{p} + (I_{zz} - I_{yy})rq + I_{xz}(\dot{r} + pq) \\ M &= I_{yy}\dot{q} + (I_{xx} - I_{zz})rp + I_{xz}(r^2 - p^2) \\ N &= I_{zz}\dot{r} + (I_{yy} - I_{xx})qp + I_{xz}(\dot{p} - qr) \end{aligned} \quad (53.39)$$

$$\dot{\mathbf{r}} = \mathbf{R}_b^g \mathbf{V}_b^g = \begin{bmatrix} \cos \theta \cos \psi & -\cos \theta \sin \psi & \sin \phi \sin \theta \cos \psi & \sin \phi \sin \psi & \cos \phi \sin \theta \cos \psi \\ \cos \theta \sin \psi & \cos \phi \cos \psi & \sin \phi \sin \theta \sin \psi & -\sin \phi \cos \psi & \cos \phi \sin \theta \sin \psi \\ -\sin \theta & \sin \phi \cos \theta & \cos \phi \cos \theta & \cos \phi \cos \theta & \cos \phi \cos \theta \end{bmatrix} \mathbf{V}_b^g \quad (53.40)$$

$$\begin{bmatrix} \dot{\phi} \\ \dot{\theta} \\ \dot{\psi} \end{bmatrix} = \begin{bmatrix} 1 & \sin \phi \frac{\sin \theta}{\cos \theta} & \cos \phi \frac{\sin \theta}{\cos \theta} \\ 0 & \cos \phi & -\sin \phi \\ 0 & \sin \phi \frac{1}{\cos \theta} & \cos \phi \frac{1}{\cos \theta} \end{bmatrix} \begin{bmatrix} p \\ q \\ r \end{bmatrix}. \quad (53.41)$$

Analysis of the above differential equations shows that these equations are nonlinear and coupled, that is, each differential equation depends upon variables which are described by other differential equations. In general case, their analytical solutions are not known, and they can only be solved numerically. There are 12 states describing the free motion of a rigid body subject to external forces ( $\mathbf{F}_b = [X, Y, Z]^T$ ) and moments ( $\mathbf{M}_b = [L, M, N]^T$ ). In the control system design, these variables are called state variables because they completely define the state of a rigid body at any instance of time. The state variables are summarized in [Table 53.1](#) for completeness.

What remains in the description of 6DoF equations of motion is to define the external forces and moments acting on the airplane. This will be the objective of the next section.

**Table 53.1** State variables of the 6DoF equations of motion

	State variable	Definition
t4.1		
t4.2	$\mathbf{r} = [r_x, r_y, r_z]^T$	Vector of inertial position of the UAV and its components
t4.3	$\mathbf{V}_b^g = [u, v, w]^T$	Vector of inertial velocity components resolved in the body-fixed frame
t4.4	$[\phi, \theta, \psi]$	Euler angles that define the attitude of body-fixed frame with respect to the inertial frame
t4.5	$\boldsymbol{\omega} = [p, q, r]^T$	The inertial angular rates resolved in the body-fixed frame

### 53.4 Forces and Moments Acting on the Airplane

The objective of this section is to present a generalized approach to defining the external forces and moments acting on a fixed-wing UAV as functions of its states. The primary forces and moments acting on an airplane are the gravitational, thrust of the propulsion system, aerodynamic, and disturbances due to the flight in unsteady atmosphere. The most challenging task here is in defining the aerodynamic forces and moments resulting from the air–body interaction. Although the aerodynamic description of airfoils defining a fixed wing is not a new subject, the varieties of shapes, aspect ratios, and aerodynamic configurations of modern fixed-wing UAVs do not allow thorough presentation of all configurations. As an example, possible aerodynamic configurations of aerodynamic surfaces include tandem, variable span wings, joined wings, twin boom, and V-tail configuration, just to name a few. However, a generalization is possible. An interested reader is referred to the most relevant survey (Mueller and DeLaurier 2003) of aerodynamics of small UAV that describes the modeling approaches and their limitations.

#### 53.4.1 Gravitation

Assuming that the flight altitude is negligible in comparison to the radius of the Earth, it is sufficient to consider the gravity’s magnitude constant. Then, the effect of the Earth’s gravitation can be naturally modeled in the body-carried frame by the force applied to the CG of the UAV of mass  $m$ ; the gravitational force is proportional to the gravitational constant  $g$  and is called the weight of the UAV

$$\mathbf{F}_u^{gr} = \begin{bmatrix} 0 \\ 0 \\ mg \end{bmatrix}. \quad (53.42)$$

Before substituting this force expression into the equations of motion (53.39), it needs to be resolved in the body frame. The inertial to body rotation  $R_u^b$  enables this transformation:

$$\mathbf{F}_b^{gr} = R_u^b \begin{bmatrix} 0 \\ 0 \\ mg \end{bmatrix} = mg \begin{bmatrix} -\sin \theta \\ \sin \phi \cos \theta \\ \cos \theta \cos \phi \end{bmatrix}. \quad (53.43)$$

Assuming that the frame  $\{b\}$  origin is chosen at the CG and since the gravitational force acts through the CG of the airplane, the corresponding moment contribution is zero,  $\mathbf{M}_b^{gr} = [0, 0, 0]^T$ .

### 53.4.2 Propulsion

The configuration of the propulsion system of modern fixed-wing UAVs varies greatly. The architectures can be categorized by the number of engines, their type, and their installation arrangement in the airframe. A thorough review of the existing configurations along with some future projections and trends in the modern and future UAV systems can be found in reference (OSD 2001). However, what is common across all possible configurations is that the vector of thrust in all systems is set parallel to the existing axes of symmetry; the thrust vectoring is not a common feature of fixed-wing UAVs yet.

The thrust is naturally represented in the body-fixed reference system. The direction of the thrust vector  $\mathbf{F}_b^{tr}$  is usually fixed and lies in the plane of symmetry or is parallel to it; however, it may not be aligned with the longitudinal  $x_b$ -axis. If the orientation of the thrust vector  $\mathbf{F}_b^{tr}$  varies in its reference to the airframe, then a separate coordinate system analogous to the wind axes should be defined, thus introducing the required rotation of the thrust vector to the body-fixed coordinate system. It is a common design requirement that the installation of multiple engines should not introduce any unbalanced moments, thus not inducing any loss of control efforts for the UAV stabilization. For the analysis of a nominal flight regime, the thrust vector  $\mathbf{F}_b^{tr}$  is considered fixed with respect to the body-fixed frame.

For the sake of simplicity, consider a typical fixed-wing UAV architecture where the installation of one or multiple engines results in the cumulative thrust vector  $\mathbf{F}_b^{tr}$  passing through the CG and the only moment being the torque generated primarily by the reactive force from the rotating propeller; depending on the type and the power of the propulsion system, there might be three more components (Illman 1999) of the torque, namely, the spiraling slipstream, the gyroscopic precession, and the asymmetric propeller loading (“P-factor”). Thus, in the case of a typical UAV, the net force  $X_{tr}$  of thrust in  $x_b$  direction and the moment  $L$  around  $x_b$  axis can be considered proportional to the thrust control command  $\delta_{tr}$ . Moreover, thrust characteristics of most conventional engines are always functions of the air density and the airspeed. Thus, the contributing force and moment resulting from the propulsion system can be presented as follows:

$$\mathbf{F}_b^{tr} = \begin{bmatrix} F_{tr}(V_a, h, \delta_{tr}) \\ 0 \\ 0 \end{bmatrix}; \mathbf{M}_b^{tr} = \begin{bmatrix} M_{tr}(V_a, h, \delta_{tr}) \\ 0 \\ 0 \end{bmatrix}. \quad (53.44)$$

769 A particular example of modeling the propulsion force for the case of a micro UAV  
770 can be found in Beard and McLain (2012).

### 771 53.4.3 Unsteady Atmosphere

772 In the previous discussion of the wind frame, it was assumed that the wind  $\mathbf{V}_u^w$   
773 defined in the LTP frame is constant; thus, the velocities are related by the “wind  
774 triangle” equation  $\mathbf{V}_u^a = \mathbf{V}_u^g - \mathbf{V}_u^w$ .

775 The most common approach (McRuer et al. 1999) in wind modeling is to  
776 consider the two components contributing to the wind. The first component  $\mathbf{V}_u^{wsteady}$   
777 defines the steady wind resolved in the inertial frame, and therefore it can be  
778 presented by the measurements in the LTP frame. The second component  $\mathbf{V}_b^{wgust}$   
779 is stochastic, which represents the short-period disturbances or gusts resolved in the  
780 body-fixed frame. Since the equations of motion are written in the body-fixed frame,  
781 then

$$782 \quad \mathbf{V}_b^w = R_u^b \mathbf{V}_u^{wsteady} + \mathbf{V}_b^{wgust}. \quad (53.45)$$

783 From the components of the wind and the UAV velocity, both resolved in the body  
784 frame, it is therefore possible to find the body frame components of the air velocity  
785 as

$$786 \quad \mathbf{V}_b^a = \begin{bmatrix} u_a \\ v_a \\ w_a \end{bmatrix} = \begin{bmatrix} u \\ v \\ w \end{bmatrix} - R_u^b \begin{bmatrix} u^{wsteady} \\ v^{wsteady} \\ w^{wsteady} \end{bmatrix} - \begin{bmatrix} u^{wgust} \\ v^{wgust} \\ w^{wgust} \end{bmatrix}. \quad (53.46)$$

787 These body frame components of the air velocity enable straightforward calculation  
788 of the airspeed and the angles of attack and sideslip as in (53.22).

789 Modeling of the stochastic and steady components of wind is based primarily  
790 on a history of experimental observations expressed using linear filters. The most  
791 widely used techniques are represented by von Karman and Dryden wind turbulence  
792 models (Hoblit 2001). Both methods are well supported with their numerical  
793 implementations.

### 794 53.4.4 Aerodynamics

795 Aerodynamic forces and moments depend on the interaction of an aircraft with  
796 the airflow, which may also be in motion relative to the Earth. However, for the  
797 purpose of representing the nominal aerodynamic effects, the large-scale motion of  
798 the atmosphere is not critical and therefore will be considered constant; in fact, it  
799 will only affect the navigation of the UAV.

800 The small perturbation theory (Ashley and Landahl 1985) is one of the ap-  
801 proaches used in describing the aerodynamic interaction of a given aerodynamic  
802 shape with airflow. The perturbation in aerodynamic forces and moments are  
803 functions of variations in state variables and control inputs. The control inputs here

are the deflections of the control surfaces of an airplane that modify the airflow around the body, thus generating the desired aerodynamic effects. The nomenclature of the control surfaces and their control mechanization depends on the particular aerodynamic composition of the airplane. Nevertheless, the principles describing the effects of the control surface deflection on the generated forces and moments are the same. Consider the following control effectors of a classical aerodynamic configuration: the elevator, the aileron, and the rudder (see Fig. 53.9). In this configuration, the ailerons are used to control the roll angle  $\phi$ , the elevator is used to control the pitch angle  $\theta$ , and the rudder controls the yaw angle  $\psi$ .

Their deflections are denoted as  $\delta_a$  for the aileron,  $\delta_e$  for the elevator, and  $\delta_r$  for the rudder. The positive deflection of a control surface is defined by applying the right-hand rule to the rotation axis of the surface. The positive direction of the aileron, elevator, and rudder deflections is also depicted in Fig. 53.9.

Deflection of the control surfaces modifies the pressure distribution around the control surfaces or the entire body thus producing corresponding forces. The forces acting with respect to the CG of the body result in aerodynamic moments. For example, deflecting the elevator primarily changes the pitching moment acting on the airplane. In turn, this results in changing the angle of attack of the wing that increases the lifting power of the airplane. The calculation of aerodynamic characteristics of one or more lifting surfaces with variable deflections of the control surfaces at various attitudes with respect to the airflow can be accomplished by utilizing well-developed linear panel methods (Hess 1990; Henne 1990) conveniently implemented in various software packages (Fearn 2008; Kroo 2012).

The panel methods capture the effect of pressure distribution in the form of parameterized forces and moments versus the angles of attack and sideslip, and airspeed; they play a role of states here. For example, considering the longitudinal plane, the effect of aerodynamic pressure acting on a fixed wing can be modeled using a total force  $\mathbf{F}_b^\Sigma$  and pitching moment  $\mathbf{M}_b^\Sigma$  acting on the wing both resolved in the body frame. It is common to project the total force to the wind axes, thus resulting in the lift  $F_{lift}$  and drag  $F_{drag}$  force components. Figure 53.10

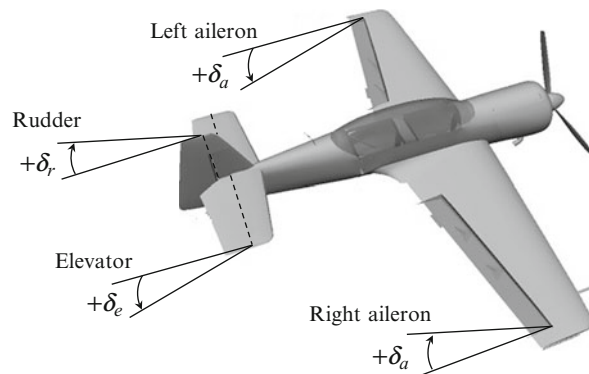
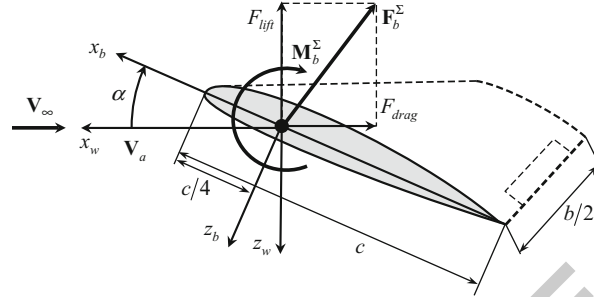


**Fig. 53.9** Control surfaces of a classical aerodynamic configuration

**Fig. 53.10** Definition of the lift and drag forces and the pitching moment in the wind frame



demonstrates the approach to modeling aerodynamic effects in the wind and body-fixed frames with respect to the vector of free airstream  $V_\infty$ .

As shown in Fig. 53.10, the lift  $F_{lift}$  and drag  $F_{drag}$  forces act in the wind frame and are applied at the aerodynamic center of the lifting surface that is located at the quarter-chord point ( $c$  is the length of the mean aerodynamic chord). The pitching component  $M$  of moment  $M_b^\Sigma$  acts around the aerodynamic center. Then, the values of forces and moments are represented in a form connecting a number of surface-specific parameters and the states in the following form:

$$\begin{aligned} F_{lift} &= \frac{1}{2} \rho V_a^2 S C_L \\ F_{drag} &= \frac{1}{2} \rho V_a^2 S C_D, \\ M &= \frac{1}{2} \rho V_a^2 S c C_m \end{aligned} \quad (53.47)$$

where  $C_L$ ,  $C_D$ ,  $C_m$  are the nondimensional aerodynamic coefficients (to be parameterized),  $S$  is the planform area of the wing surface, and  $c$  and  $b$  are the mean aerodynamic chord and the wing span. The same approach is applied to each of the aerodynamic surfaces comprising the airplane. Then by using the parallel axis theorem (Goldstein 1980), the elementary moments from all the lifting and control surfaces can be transferred to the CG of the rigid body, thus resolving the actions with respect to one unifying center.

It is common practice to consider the total aerodynamic forces and moments in projections to the longitudinal and lateral planes of the airplane. The benefit of this approach is in the simplicity of representing the aerodynamic effects and in providing a natural ground for the nonlinear model decomposition at the next step of the control system design. Thus, the longitudinal forces and moments (53.47) consist of lift, drag, and pitching moment acting in the vertical plane of symmetry. The lateral side force  $F_{side}$ , yawing  $N$ , and rolling  $L$  moments are caused by the asymmetric airflow around the airplane and control surfaces deflection; the asymmetry can be caused by the side wind or intentional deflection of the rudder. For the majority of fixed-wing UAVs, the key states that define the parameterization



**Table 53.2**

Parameterization of longitudinal and lateral aerodynamics

Longitudinal channel	Lateral channel
$F_{drag} = 1/2 \rho V_a^2 S C_D(\alpha, q, \delta_e)$	$F_{side} = 1/2 \rho V_a^2 S C_Y(\beta, p, r, \delta_r, \delta_a)$
$F_{lift} = 1/2 \rho V_a^2 S C_L(\alpha, q, \delta_e)$	$L = 1/2 \rho V_a^2 S b C_l(\beta, p, r, \delta_r, \delta_a)$
$M = 1/2 \rho V_a^2 S c C_M(\alpha, q, \delta_e)$	$N = 1/2 \rho V_a^2 S b C_n(\beta, p, r, \delta_r, \delta_a)$

of the aerodynamic coefficient are the angle of attack  $\alpha$ , the sideslip  $\beta$ , body rates  $[p, q, r]$ , and the controls which are the surface deflections  $[\delta_e, \delta_r, \delta_a]$ . The most general functional form of the longitudinal and lateral aerodynamics can be presented as follows (Table 53.2):

AU9

Without delving deeper into the intricacies of aerodynamic parameterization, it is sufficient to demonstrate the final form of forces and moments defined in the wind coordinate frame:

• Longitudinal plane

$$\begin{aligned}
 F_{drag} &= 1/2 \rho V_a^2 S \left( C_{D_0} + C_D^\alpha \alpha + C_D^q \frac{c}{2V_a} \cdot q + C_D^{\delta_e} \cdot \delta_e \right) \\
 F_{lift} &= 1/2 \rho V_a^2 S \left( C_{L_0} + C_L^\alpha \alpha + C_L^q \frac{c}{2V_a} \cdot q + C_L^{\delta_e} \cdot \delta_e \right) \\
 M &= 1/2 \rho V_a^2 S c \left( C_{M_0} + C_M^\alpha \alpha + C_M^q \frac{c}{2V_a} \cdot q + C_M^{\delta_e} \cdot \delta_e \right)
 \end{aligned} \tag{53.48}$$

869

• Lateral plane

$$\begin{aligned}
 F_{side} &= 1/2 \rho V_a^2 S \left( C_{Y_0} + C_Y^\beta \beta + C_Y^p \frac{b}{2V_a} \cdot p + C_Y^r \frac{b}{2V_a} \cdot r + C_Y^{\delta_r} \cdot \delta_r + C_Y^{\delta_a} \cdot \delta_a \right) \\
 L &= 1/2 \rho V_a^2 S b \left( C_{l_0} + C_l^\beta \beta + C_l^p \frac{b}{2V_a} \cdot p + C_l^r \frac{b}{2V_a} \cdot r + C_l^{\delta_r} \cdot \delta_r + C_l^{\delta_a} \cdot \delta_a \right) \\
 N &= 1/2 \rho V_a^2 S b \left( C_{n_0} + C_n^\beta \beta + C_n^p \frac{b}{2V_a} \cdot p + C_n^r \frac{b}{2V_a} \cdot r + C_n^{\delta_r} \cdot \delta_r + C_n^{\delta_a} \cdot \delta_a \right)
 \end{aligned} \tag{53.49}$$

871

The presented parameterization is a simple linear approximation of the aerodynamics given by the Taylor series expansion taken with respect to the given trim conditions. The coefficients  $C_{f/m}^{state}$  are the nondimensional partial derivatives of the corresponding forces and moments (denoted in the subscript) defined with respect to the corresponding state or control (denoted in the superscript). The coefficients with zero in the subscript denote the forces and moments calculated when all states, including the control surface deflection, are zero; for example,  $C_{l_0}$  denotes the roll moment coefficient estimated at  $\beta = p = r = 0$  and  $\delta_r = \delta_a = 0$ . The common naming convention suggests that those derivatives defined with respect to states  $[\alpha, \beta, p, q, r]$  are called the stability derivatives and those with respect to controls  $[\delta_e, \delta_r, \delta_a]$  are called the control derivatives. The static stability of an aircraft

with respect to disturbances in some variable is directly reflected in the sign of a particular derivative. For example, the sign of  $C_M^\alpha$  should be negative to guarantee static stability in pitching motion, while the sign of  $C_N^\beta$  should be positive for the directional static stability.

Each of the presented coefficients is usually a function of states. The precision requirement of the linear parameterization greatly depends on the operational envelop of the UAV and its intended use; the higher the maneuverability of the UAV, the more terms necessary to accurately represent the aerodynamics. Each of the coefficients has very intuitive physical meaning and is usually studied separately. An interested reader is referred to Beard and McLain (2012) for a detailed discussion of the aerodynamic coefficients of small and micro fixed-wing UAVs.

One last step needs to be performed before the aerodynamics (53.48) and (53.49) defined in the wind coordinates can be plugged into the equations of motion (53.38) and (53.39) resolved in the body-fixed frame. The transformation (53.19) from the wind to the body frame serves this purpose.

Therefore, the total forces and moments acting on the fixed-wing UAV can be presented as follows:

$$\begin{bmatrix} X \\ Y \\ Z \end{bmatrix} = R_u^b \begin{bmatrix} 0 \\ 0 \\ mg \end{bmatrix} + \begin{bmatrix} F_{tr}(V_a, h, \delta_{tr}) \\ 0 \\ 0 \end{bmatrix} + \frac{1}{2} \rho V_a^2 S \cdot R_w^b \begin{bmatrix} C_D(\alpha, q, \delta_e) \\ C_Y(\beta, p, r, \delta_r, \delta_a) \\ C_L(\alpha, q, \delta_e) \end{bmatrix} \quad (53.50)$$

$$\begin{bmatrix} L \\ M \\ N \end{bmatrix} = \begin{bmatrix} M_{tr}(V_a, h, \delta_{tr}) \\ 0 \\ 0 \end{bmatrix} + \frac{1}{2} \rho V_a^2 S \cdot \begin{bmatrix} b C_l(\beta, p, r, \delta_r, \delta_a) \\ c C_m(\alpha, q, \delta_e) \\ b C_n(\beta, p, r, \delta_r, \delta_a) \end{bmatrix}. \quad (53.51)$$

### 53.5 Accounting for the Earth Rotation Rate

The complete set of 6DoF equations of motion presented above is an approximation of the rigid body kinematics and dynamics and is valid as long as the assumption of the flat Earth model satisfies the task at hand. During the high-speed flight or in long-duration and extended range missions, the precision of the derived states will suffer from omitting the sidereal rate of the rotating Earth. The key reason for the error is in the accumulation over time of the Coriolis and centripetal accelerations induced by the rotating Earth. Thus, the following derivation outlines how the Earth rotation can be accounted for in the definition of the inertial velocity and acceleration vectors.

First, consider the ECI as the true inertial frame  $\{i\}$ . Next, by using the simplifying properties of defining the free motion of a rigid body with respect to the CG and utilizing the Coriolis theorem, resolve the absolute time derivative of the CG position vector  $\mathbf{r}_i^{cg}$  in the true inertial frame as follows:

$$\mathbf{V}_i^{cg} = \dot{\mathbf{r}}_i^{cg} = \mathbf{V}_e^{cg} + \boldsymbol{\Omega}_i^e \times \mathbf{r}_i^{cg}. \quad (53.52)$$

918 Taking the second time derivative and assuming that that the sidereal rate of the  
919 Earth rotation is constant ( $\dot{\Omega}_i^e = 0$ ) results in

$$\begin{aligned}\dot{\mathbf{V}}_i^{cg} &= \dot{\mathbf{V}}_b^{cg} + \boldsymbol{\omega} \times \mathbf{V}_e^{cg} + \Omega_i^e \times \dot{\mathbf{r}}_i^{cg} = \dot{\mathbf{V}}_b^{cg} + \boldsymbol{\omega} \times \mathbf{V}_e^{cg} + \Omega_i^e \times (\mathbf{V}_e^{cg} + \Omega_i^e \times \mathbf{r}_i^{cg}) \\ &= \dot{\mathbf{V}}_b^{cg} + (\boldsymbol{\omega} + \Omega_i^e) \times \mathbf{V}_e^{cg} + \Omega_i^e \times (\Omega_i^e \times \mathbf{r}_i^{cg})\end{aligned}\quad (53.53)$$

920  
921 In (53.53), the  $\boldsymbol{\omega}$  denotes the vector of inertial angular velocity resolved in the  
922 body frame, and  $\mathbf{V}_b^{cg}$  is the same as  $\mathbf{V}_b^g = \mathbf{V}_b^g$ . The equation (53.52) updates  
923 the kinematic dead reckoning equation in (53.39), while the vector of inertial  
924 acceleration in (53.53) should be used in the application of the second Newtonian  
925 law.

926 Applying the angular velocities addition theorem, the vector  $\boldsymbol{\omega}$  can be repre-  
927 sented as a sum of the angular velocity vector  $\boldsymbol{\omega}_n^b$  of body frame  $\{b\}$  resolved in the  
928 body-carried frame  $\{n\}$ , the angular velocity vector  $\boldsymbol{\omega}_e^n$  of body-carried frame  $\{n\}$   
929 resolved in ECEF frame  $\{e\}$ , and the sidereal rate of the Earth rotation vector  $\Omega_i^e$   
930 resolved in the true inertial frame  $\{i\}$ . Thus, the last equation can be also written as

$$\dot{\mathbf{V}}_i^{cg} = \dot{\mathbf{V}}_b^{cg} + (\boldsymbol{\omega}_n^b + \boldsymbol{\omega}_e^n + 2\Omega_i^e) \times \mathbf{V}_e^{cg} + \Omega_i^e \times (\Omega_i^e \times \mathbf{r}_i^{cg}). \quad (53.54)$$

932 What remains is to define the elements of (53.54) that enable calculation of the  
933 vector cross products.

934 As before, the term  $2\Omega_i^e \times \mathbf{V}_e^{cg}$  is the Coriolis, and the term  $\Omega_i^e \times (\Omega_i^e \times \mathbf{r}_i^{cg})$ , is  
935 the centripetal accelerations. The angular velocity vector  $\boldsymbol{\omega}_e^n$ , can be obtained from  
936 the geodetic latitude ( $\phi$ ) and longitude ( $\lambda$ ) rates, which in turn can be calculated  
937 from the NED components of  $\mathbf{V}_e^{cg} = [V_N, V_E, V_D]^T$ . The transformation of rates of  
938 the geodetic system ( $\dot{\phi}, \dot{\lambda}$ ) to the body-carried stabilized frame  $\{n\}$  can be obtained  
939 similarly to (53.10) by a left-handed rotation around the east axis through the latitude  
940 angle  $\phi$

$$\boldsymbol{\omega}_e^n = \begin{bmatrix} 0 \\ -\dot{\phi} \\ 0 \end{bmatrix} + \begin{bmatrix} \cos \phi & 0 & \sin \phi \\ 0 & 1 & 0 \\ -\sin \phi & 0 & \cos \phi \end{bmatrix} \begin{bmatrix} \dot{\lambda} \\ 0 \\ 0 \end{bmatrix}. \quad (53.55)$$

942 The rate of change of latitude and longitude can be calculated from the  $V_n$  northern  
943 and  $V_e$  eastern components of the velocity vector as follows:

$$\dot{\phi} = \frac{V_n}{r_m + h}, \quad \dot{\lambda} = \frac{V_E}{(r_n + h) \cos \phi}, \quad (53.56)$$

945 where  $h$  is the height of CG above the reference oblate spheroid and

$$r_m = \frac{r_e(1 - \varepsilon^2)}{(1 - \varepsilon^2 \sin^2 \phi)^{\frac{3}{2}}}, \quad r_n = \frac{r_e}{\sqrt{1 - \varepsilon^2 \sin^2 \phi}}$$

are the estimates of the reference spheroid radius in the meridian and normal directions at given latitude and longitude. Substituting (53.56) into the (53.55) results in the estimate of  $\omega_e^n$  as follows:

$$\omega_e^n = \left[ \frac{V_E}{r_n + h}, -\frac{V_N}{r_m + h}, -\frac{V_E}{r_n + h} \tan \phi \right]^T. \quad (53.57)$$

Observe that the Earth sidereal rotation vector  $\Omega_i^e$  has only one component in ECEF frame  $\Omega_i^e = [0, 0, \Omega_i^e]^T$ . Resolving for convenience  $\Omega_i^e$  in the  $\{n\}$  frame by a single  $\varphi$  rotation produces

$$\Omega_i^n = [\Omega_i^e \cos \phi, 0, -\Omega_i^e \sin \phi]^T, \quad (53.58)$$

thus completing the definition of all terms in (53.54). Obviously, the result of substituting of all the vectors into (53.54) is cumbersome; however it demonstrates how the Earth sidereal rate can be accounted for.

The corresponding linear and angular momentum equations can be obtained by applying the second Newtonian law; the procedure is similar to the simplified case presented above and resulted in the (53.26) and (53.32). Utilizing the same set of assumptions (A1–A2) and resolving all the external forces and moments with respect to the CG in the body frame results in the same angular momentum equation; however, the kinematic and the linear momentum equations need to be modified. Applying the second Newtonian law to the linear motion of the CG and accounting for a new result in (53.52) and (53.53) gives

$$\mathbf{V}_i^{cg} = R_b^e \mathbf{V}_b^{cg} + \Omega_i^e \times \mathbf{r}_i^{cg} \quad (53.59)$$

$$\mathbf{F}_b = m [\dot{\mathbf{V}}_b^{cg} + (\omega + \Omega_b^e) \times R_b^e \mathbf{V}_b^{cg} + \Omega_b^e \times (\Omega_b^e \times R_b^e \mathbf{r}_i^{cg})], \quad (53.60)$$

where  $\mathbf{F}_b$ , as before, is the sum of all externally applied forces applied at CG resolved in the body frame. Equations (53.59) and (53.60) are the new relations derived in a true inertial frame  $\{i\}$ , thus accounting for the rotating Earth.

To give a reader a sense of numerical significance of the resulting acceleration, the following numerical example compares the contribution of the Coriolis and the centripetal terms with an assumption that a UAV is at the constant altitude in the wing-level flight due east and is not maneuvering; therefore,  $\omega_n^b = 0$  and  $\mathbf{V}_e^{cg} = [0, V_E, 0]^T$ . In these conditions, the centripetal term becomes equal to the Coriolis term at the speed of 914 m/s. In turn, when at the equator latitude, the third vertical component of the Coriolis acceleration is about  $0.27 \text{ m/s}^2$ , that is, 2.7 % of the acceleration due to gravity ( $9.8 \text{ m/s}^2$ ). Thus, the applicability of the simplifying flat Earth assumption becomes justified for a case of a short-duration and relatively low-speed flight of an airplane. Therefore, this new set of equations should be used when accurate modeling is required for a UAV moving faster than 600 m/s over the Earth or when long distance and duration navigation is considered.

## 984 53.6 Conclusion

985 The objective of this chapter was to provide a review of the theoretical material  
 986 required to enable accurate mathematical representation of the free and controlled  
 987 motion of a generic fixed-wing UAV modeled as a rigid body. The key building  
 988 blocks presented were the coordinate frames and their transformations, kinematics  
 989 of rotation, dynamics of motion, and the definition of forces and moments acting  
 990 on the airplane. The kinematics of spatial rotation is what connects the three  
 991 building blocks of the “kinematics–dynamics–actions” triad. In addition to the 6DoF  
 992 equations of motion describing the kinematics and dynamics of a rigid body motion,  
 993 the tools and methods developed in this chapter contribute significantly into the UAV  
 994 flight dynamics, system identification, control, guidance, and navigation.

## 995 References

- 996 H. Ashley, M. Landahl, *Aerodynamics of Wings and Bodies (Dover Books on Aeronautical*  
 997 *Engineering)* (Dover Publications, New York, 1985)  
 998 R. Beard, T. McLain, *Small Unmanned Aircraft: Theory and Practice* (Princeton University Press,  
 999 Princeton, 2012)  
 1000 B. Etkin, L.D. Reid, *Dynamics of Flight: Stability and Control*, 3rd edn. (Wiley, New York, 1995)  
 1001 R.L. Fearn, Airfoil aerodynamics using panel methods. *Math. J. (Wolfram Research)* **10**(4), 15  
 1002 (2008)  
 1003 H. Goldstein, *Classical Mechanics*, 2nd edn. (Addison-Wesley, Reading, 1980)  
 1004 P. Henne, *Applied Computational Aerodynamics (Progress in Astronautics and Aeronautics)*  
 1005 (AIAA, Washington, DC, 1990)  
 1006 J.L. Hess, Panel methods in computational fluid dynamics. *Ann. Rev. Fluid Mech.* **22**, 255–274  
 1007 (1990)  
 1008 F. Hoblit, *Gust Loads on Aircraft: Concepts and Applications* (AIAA Education Series, Washing-  
 1009 ton, DC, 2001)  
 1010 P.E. Illman, *The Pilot's Handbook of Aeronautical Knowledge* (McGraw-Hill Professional,  
 1011 New York, 1999)  
 1012 G.H. Kaplan, *The IAU Resolutions on Astronomical Constants, Time Scales, and the Fundamental*  
 1013 *Reference Frames*, vol. circular no. 163 (United States Naval Observatory, Washington, DC,  
 1014 1981)  
 1015 I. Kroo, LinAir 4. A nonplanar, multiple lifting surface aerodynamics program. Desktop Aeronau-  
 1016 tics (2012). <http://www.desktop.aero/linair.php>. Accessed 10 Apr 2012  
 1017 D. McRuer, I. Ashkenas, D. Graham. *Aircraft Dynamics and Automatic Control* (Princeton  
 1018 University Press, Princeton, 1999)  
 1019 T.J. Mueller, J.D. DeLaurier, Aerodynamics of small vehicles. *Ann. Rev. Fluid Mech* **35**, 89–111  
 1020 (2003)  
 1021 R. Murray, Z. Li, S. Sastry, *A Mathematical Introduction to Robotic Manipulation*, vol. 1 (CRC  
 1022 Press, Boca Raton, 1994)  
 1023 OSD, *Unmanned Aerial Vehicles Roadmap 2000–2025* (Office of the Secretary of Defence,  
 1024 Washington, DC, 2001)  
 1025 R.M. Rogers, *Applied Mathematics in Integrated navigation Systems*, 2nd edn. (AIAA, Reston,  
 1026 2003)  
 1027 M.D. Shuster, A survey of attitude representations. *J. Astronaut. Sci.* **41**(4), 439–517 (1993)

AU10

AU11

### Author Query Form

**Handbook of Unmanned Aerial Vehicles**  
**Chapter No. 53**

Query Refs.	Details Required	Author's response
AU1	Please check if author affiliation is okay.	
AU2	All occurrences of “DOF” have been changed to “DoF.” Please check if okay.	
AU3	Please check if edit to sentence starting “It is important. . .” is okay.	
AU4	“Rodriguez” has been changed to “Rodrigues.” Please check if okay.	
AU5	Please check if edit to sentence starting “Depending on. . .” is okay.	
AU6	Please check if edit to sentence starting “The ECI. . .” is okay.	
AU7	Please check if edit to sentence starting “Assuming that. . .” is okay.	
AU8	Please check if edit to the sentence starting “Then the transformation . . .” is okay.	
AU9	Please check if inserted citation for Table 53.2 is okay.	
AU10	Please check if updated publisher location for Ashley and Landahl (1985), Beard and McLain (2012), Etkin and Reid (1995), Goldstein (1980), Henne (1990), Hoblit (2001), Illman (1999), McRuer et al. (1999), and Murray et al. (1994) are okay.	
AU11	Please check if updated volume number for Mueller and DeLaurier (2003) is okay.	